ELSEVIER

Journal of Archaeological Science 31 (2004) 1137–1160

Journal of Archaeological SCIENCE

http://www.elsevier.com/locate/jas

Review article

Raman microscopy in archaeological science

Gregory D. Smith, Robin J.H. Clark *

Christopher Ingold Laboratories, University College London, 20 Gordon Street, London WC1H 0AJ, UK

Received 7 February 2003; received in revised form 28 August 2003

Abstract

Improvements in the instrumentation for dispersive and interferometric Fourier transform (FT) Raman microscopy have overcome many of the earlier limitations of these techniques, thus opening the way for their widespread and routine utilisation in archaeometry laboratories. The use of Raman spectroscopy for identifying and studying archaeological materials has flourished in recent years, but the resulting articles have seldom been published in the archaeology literature, thus limiting their impact on the field. Therefore, this article covers concisely the theory and instrumentation of Raman microscopy and then comprehensively reviews the many applications of this technique in archaeometric research. The significant advances made in archaeological science through the use of Raman microscopy are highlighted, but many areas requiring further research, such as the generation of more extensive and reliable spectral libraries and the surmounting of obstacles in the analysis of certain classes of historical materials, are also revealed.

Keywords: Archaeology; Archaeometry; Art; Vibrational spectroscopy; Raman microscopy

1. Introduction

Over the past decade, advances in instrumentation for generating, sorting, and detecting Raman scattered light have overcome many of the limitations that had earlier allowed infrared (IR) techniques to eclipse Raman spectroscopy as a laboratory tool for vibrational spectroscopy [100]. These obstacles included the intrinsic weakness of the Raman scattering phenomenon, the scale and cost of the requisite instrumentation, and the tendency of the weak Raman signal to be overwhelmed by broadband fluorescence from some samples. The introduction of high throughput optical configurations, efficient Rayleigh rejection filters, and high quantum yield charge-coupled device (CCD) detectors have improved tremendously the sensitivity of modern Raman instruments [100] while simultaneously reduced their cost [92]. Furthermore, near-IR (NIR) lasers used in conjunction with dispersive or interferometric spectrometers have diminished the limitations imposed by fluorescent samples [93,94]. The coupling of a Raman spectrometer to an optical microscope has further increased the versatility of the method by allowing the selective analysis of components of heterogeneous samples on a micrometre scale and by reducing greatly the amount of sample required from precious materials. With these numerous improvements, Raman microscopy has become a proven analytical technique in all areas of scientific research [136], and its application to the identification and study of artwork and artefacts has begun to flourish.

Most of this archaeometric research has arisen from a small community of chemical spectroscopists, which includes the present authors, who have partly turned their attention to the analysis of historical materials. Consequently, few of these studies have appeared in the archaeometry literature, but rather in specialist chemistry and spectroscopy journals. The present article seeks to rectify this situation by presenting some technical information on Raman microscopy and then comprehensively reviewing its applications in archaeometry. The same circumstances that have motivated the writing of this review existed for the use of Raman microscopy in art history and conservation science, and a comparable

* Corresponding author. Tel.: +44-171-387-7050; fax: +44-171-504-4603.

E-mail address: r.j.h.clark@ucl.ac.uk (R.J.H. Clark).

0305-4403/$ - see front matter © 2004 Elsevier Ltd. All rights reserved.
doi:10.1016/j.jas.2004.02.008

review featuring applications in these areas has already appeared and will be of interest to those seeking a complete catalogue of Raman applications to the study of historical materials [128].

2. Raman spectroscopy

Raman spectroscopy probes molecular and crystal lattice vibrations and therefore is sensitive to the composition, bonding, chemical environment, phase, and crystalline structure of the sample material. These characteristics make it an exceptional method for unambiguously identifying materials in any physical form: gases, liquids, solutions, and crystalline or amorphous solids. Although this is similar to the role that IR spectroscopy has played in the laboratory since the 1940s, the phenomena on which the Raman and IR techniques rely are very different from one another, and the instrumentation is also distinct. Although these topics have been treated in detail elsewhere [94,103], a brief discussion of the basic principles of the Raman technique, its requisite instrumentation, and many advantages is desirable here in order to facilitate the understanding of the applications that follow.

2.1. The Raman scattering phenomenon

Fig. 1 depicts schematically the simplest classical view of the Raman scattering process. A sample is illuminated with a monochromatic photon beam (frequency ν_0), most of which are either absorbed, reflected, or transmitted by the sample. A small fraction, however, interacts with the sample via the oscillating electric field of the incoming photons. The molecules so affected

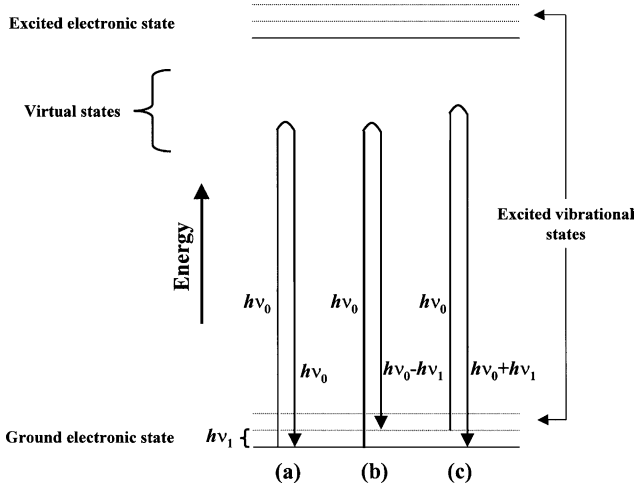

Fig. 1. Energy level diagram showing the concerted excitation–relaxation phenomena responsible for (a) Rayleigh, (b) Stokes, and (c) anti-Stokes Raman scattering.

can—in the simplest possible view of the process—be considered to reside in 'virtual' excited states, which are highly unstable, decaying instantaneously to the ground state by one of three different processes. Most of the incoming photons that are scattered do so elastically, a phenomenon referred to as Rayleigh scattering (Fig. 1(a)), whereby the emission of a photon of the same energy allows the molecule to relax to its ground vibrational state. Rayleigh scattering, therefore, bears no information regarding the vibrational energy levels of the sample. However, for a diatomic molecule with a vibrational frequency ν_1, an even smaller proportion (approximately 1 in 10^6) is scattered inelastically at energies both below, $h\nu_0 - h\nu_1$, and above, $h\nu_0 + h\nu_1$, that of the Rayleigh photons, thereby generating a set of frequency-shifted 'Raman' photons. The energy differences of the Stokes ($-h\nu_1$, Fig. 1(b)) and anti-Stokes ($+h\nu_1$, Fig. 1(c)) Raman photons with respect to the excitation energy ($h\nu_0$) relate to either energy lost, or more rarely gained, by a scattered photon as the molecule returns to either a higher or lower vibrational level, respectively. These vibrational energy levels are therefore probed *indirectly* by Raman spectroscopy, but are the same as those probed *directly* by IR absorption spectroscopy. Although the vibrational information obtainable by Raman spectroscopy is *similar* to that obtained by IR spectroscopy, it is not *identical*, but rather *complementary*, owing to the different selection rules governing vibrational Raman scattering (mandatory change in polarisation) and IR absorption (mandatory change in dipole moment). The detailed theory of the Raman effect in terms of the Kramers–Heisenberg dispersion formula is set out elsewhere [35,103].

Fig. 2 shows the Raman spectra of three different lead oxides. Since the energy differences, $h\nu_i$, of Raman photons relative to the excitation energy are characteristic of the vibrational energy levels probed, i.e. they scale directly with the wavenumbers (cm^{-1}, the number of waves per centimetre) of bands in IR spectroscopy, the Raman spectrum is conventionally plotted in terms of this Raman shift in wavenumbers (lower abscissa) rather than as the absolute wavenumber of the Raman photons themselves (upper abscissa). Anti-Stokes Raman scattering requires molecules to be originally in an excited rather than the ground vibrational state (see Fig. 1(c)), a less probable occurrence, and so the intensities of anti-Stokes Raman bands are very weak but temperature dependent (Boltzmann law). Consequently, Raman spectra reported in the literature commonly include only the Stokes portion as shown in Fig. 2. The example spectra are derived from two structural isomers of lead(II) oxide (PbO), (a) orthorhombic yellow massicot and (b) tetragonal reddish-orange litharge, as well as from (c) red lead or minium (Pb_3O_4). These spectra were collected from single micrometre-sized grains of the mineral using the 632.8 nm (15,803 cm^{-1}) excitation line of a He–Ne

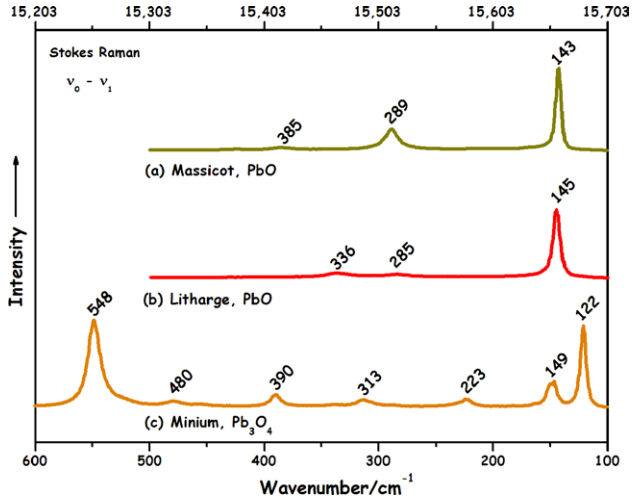

Fig. 2. Stokes Raman spectra of (a) orthorhombic massicot, (b) tetragonal litharge (both PbO), and (c) red lead or minium (Pb_3O_4). The spectra were acquired using the 632.8 nm (15,803 cm^{-1}) output of a He–Ne laser with 350 μW of power at the sample.

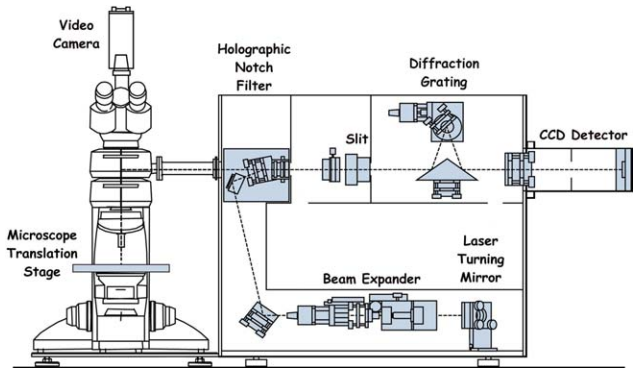

Fig. 3. Schematic of a research-grade dispersive Raman microscope (modified with permission from a drawing supplied by Renishaw plc).

laser, although Raman spectra of these minerals collected using other excitation lines are similar [25]. These lead compounds are common historical artists' materials as well as important compounds in lead pyrotechnology and corrosion. The spectra in Fig. 2 highlight the molecular specificity that is inherent in Raman spectroscopy. The molecular vibrations and crystal lattice modes are unique to each material, and even those compounds that are compositionally identical but different in crystal structure, e.g. massicot and litharge, give rise to distinct spectra.

2.2. Instrumentation

Raman instruments are becoming commonplace in academic, government, and industrial laboratories. Technological advances over the past decade have led to the production of much smaller Raman spectrometers that require only a single tabletop of laboratory space. Fig. 3 shows a modern research-grade Raman spectrometer coupled to an optical microscope; the whole instrument has a footprint of a mere 100 cm × 65 cm. Although the miniaturisation and other technological advances have greatly diminished the cost of the equipment for Raman microscopy, a research-grade system can still cost between US$70,000 and US$200,000 depending on the desired accessories [92].

One significant improvement in Raman instrumentation has been the introduction of numerous low-cost, compact, air-cooled lasers for sample excitation. The laser or lasers (not shown in Fig. 3) are positioned parallel and behind the spectrometer, and can generate a variety of different wavelengths. The efficiency of Raman scattering, however, is related to the scattered frequency (ν^4 dependence) and so, other things being equal, laser lines of higher frequency lead to the more intense Raman scattering. Nevertheless, a wide selection of laser lines is useful in optimising the experiment to the material being studied, for instance in minimising photon absorption in highly coloured materials, a process that competes with Raman scattering and can lead to photo-degradation of the sample.

The excitation beam, shown as a dashed line in Fig. 3, is directed to the microscope by beam steering optics. The microscope permits samples to be examined visually at high magnification and then allows specific areas as small as 1 μm in diameter to be analysed selectively. The reflected, Rayleigh, and Raman photons are back-collected through the same microscope objective and then directed to the spectrometer. The 180° geometry of the collection optics allows samples of any size or shape to be examined in situ and non-destructively so long as they can be placed on the microscope stage and under the microscope objective. However, this stricture is rapidly being eroded by the increasing prevalence of fibre optic accessories and side-looking microscope objectives.

The reflected and Rayleigh scattered photons represent a major source of interference in Raman spectroscopy. They must be removed so as not to saturate the detector or overwhelm the comparatively weak Raman signal. This can be done either by using a narrow-band holographic notch filter that is specific to the laser photon energy (and therefore the reflected and Rayleigh scattered photons as well), as shown in Fig. 3, or by a series of monochromators and narrow slits. The latter scheme severely restricts the optical throughput of the system and has in the past limited the application of Raman spectroscopy to only those samples that are very good Raman scatterers or ones that can endure intense laser irradiation. A double or triple monochromator system is also bulky and lacks portability, an increasingly desirable feature as more research moves to field-based laboratories. The recent introduction of

narrow-band holographic notch filters has allowed the size of the spectrometer to be greatly reduced while its optical efficiency is tremendously increased. The drawbacks, however, are that a separate expensive filter must be purchased for each excitation laser line and that the cutoff edge of the filter is often not sharp enough to prevent the rejection of Raman photons very near the wavenumber of the Rayleigh photons, i.e. within ~75–100 cm^{-1} (see Fig. 2).

Once the reflected and Rayleigh scattered light have been removed, the remaining Raman photons are either sorted spatially by a diffraction grating and detected by a CCD camera in a dispersive Raman spectrometer (see Fig. 3) or sorted interferometrically and detected by a photoconductive detector in an FT-Raman instrument. The latter is employed when one chooses to use a NIR laser in order to circumvent sample fluorescence. The neodymium–doped yttrium–aluminium–garnet (Nd^{3+}:YAG) laser operating at 1064 nm is commonly employed in this configuration. Although extremely useful in minimising fluorescence interference, the longer wavelength of this NIR laser leads to lower spatial resolution (diffraction limit) and to weaker Raman scattering (ν^4 dependence) than when a laser line in the visible region is used. The recent availability of intermediate wavelength NIR diode lasers with lasing lines (785 and 830 nm) in the sensitivity range of CCD cameras provides a valuable compromise by allowing a comparable reduction in sample fluorescence without requiring the use of interferometric systems and with less loss in spatial resolution and Raman scattering efficiency. However, many materials are strongly absorbing in the NIR spectral region, and so in all instances in which an NIR laser is employed, one must be cautious to avoid the possibility of thermally degrading the sample [93]. Ultraviolet lasers (244 and 325 nm) can also be used to avoid exciting fluorescence transitions or to photo-bleach the fluorescent contaminants from samples. Such lasers have yet to be proven in archaeometric applications though, due to concerns over potential photolytic damage to sensitive materials.

2.3. Advantages and limitations

It has been argued that Raman microscopy is the best single technique for identifying and studying inorganic solids, especially when they are heterogeneous mixtures on a micrometre scale [31,84]. The characteristics of the Raman microscope that make it so well qualified for the analysis of these materials include its molecular specificity, non-destructiveness, high spatial and spectral resolution, in situ analysis, portability, applicability to samples of large or non-uniform shape, and relative immunity to interference. The Raman technique is not without its limitations, however, and a brief mention of these is warranted. For instance, although extremely well suited for qualitative identification of a material, Raman microscopy is not easily made quantitative due to the effects of individual instrumental parameters. It is also not suitable for all forms of archaeological analysis, e.g. assaying of metal alloys or elemental fingerprinting, and nearly all pure metals are Raman silent. As mentioned previously, Raman analysis can be frustrated by naturally fluorescent organic materials, by atomic fluorescence in some materials, or by fluorophores that have become incorporated into artefacts from handling, burial, or other processes. Numerous techniques have been developed, however, to circumvent fluorescence; among these are the use of extremely long or extremely short wavelength lasers to avoid exciting the fluorescence (v. supra), the use of high magnification and confocal optics for reducing fluorescence from areas sampled unintentionally [110], and the application of spectral manipulations such as subtracted-shifted Raman analysis to eliminate the background fluorescence signal mathematically [2].

Raman spectroscopy as discussed in this review is a fingerprinting technique, thus materials are identified by comparing their characteristic vibrational spectra with those in a database. Reference libraries of Raman spectra for minerals [8,12,40,80,87], plant fibres [71], mineral and organic pigments [1,24], modern synthetic pigments [137], enamel/glaze pigments [43], archaeologically significant gums [59] and waxes [60,63], and artistic varnishes, resins, and binders [15,24,138] are available in the literature, and searchable databases of Raman spectra of thousands of organic and inorganic materials are offered commercially. Although significant progress has been made in the construction of Raman spectral databases of historical materials, many of the these 'reference' spectra originate from single examples of modern specimens. This is usually not problematic for pure natural mineral samples, but it can be for unique organic artefacts. Such samples when found in archaeological contexts are likely to be natural products of inherent chemical variability which have undergone traditional processing, subsequent aging, and possible degradation. The suitability of the modern reference spectra for identifying aged organic samples has not been fully tested. Similarly, many synthetic inorganic and organometallic materials used historically by artists, for instance verdigris ($x\mathrm{Cu(CH_3COO)_2}\cdot y\mathrm{Cu(OH)_2}\cdot z\mathrm{H_2O}$), Egyptian blue and green ($\sim\mathrm{CaCuSi_4O_{10}}$), and lead tin yellow type II ($\mathrm{PbSn_{1-x}Si_xO_3}$), are likewise variable in stoichiometry, and their Raman spectra are likely to reflect this variability. Additionally, mineral pigments can show resonance enhancement of some Raman bands [35], or can produce complex spectra if finely ground and intimately mixed with a co-mineralised species [7]. Raman band polarisation effects that depend on the orientation of a single crystal relative to the

polarized excitation beam are also evident [21,109]. These caveats are seldom incorporated into the published databases.

Even with these uncertainties, the literature spectra represent a good starting point for the identification of unknowns, and this situation is likely to improve as more analyses of historical samples are published. The 1999 name change of *The Infrared Users' Group*, an association of museum and academic vibrational spectroscopists, to *The Infrared and Raman Users' Group* (IRUG) is one such harbinger of the improvements to be expected in Raman spectral databases. IRUG now accepts Raman spectra to their popular peer reviewed database of vibrational spectra of genuine historical materials. It is hoped that the efforts of the editors and group members will generate a freely available collection of reliable and well documented Raman spectra of materials of proven authenticity.

Despite the aforementioned shortcomings, the Raman technique compares extremely well with other analytical tools commonly employed in the archaeometry laboratory for the identification of molecular solids. Several of the particularly important advantages of Raman spectroscopy are highlighted below with comparisons to other popular instrumentation. It is important to note, though, that the complexity of cultural materials often necessitates the use of multiple analytical tools for a complete and confident analysis.

As stated above, IR spectroscopy like Raman spectroscopy accesses the characteristic vibrational spectrum of a material. Although the results are similar for each technique, the use of visible photons in Raman spectroscopy and the fact that it is a scattering technique, afford it several significant advantages. The far-IR region of the spectrum ($<400\,cm^{-1}$), which contains many of the vibrational bands of inorganic materials and their crystal lattice modes, is not easily accessible by conventional IR spectroscopy, but is readily and routinely probed by Raman spectroscopy. The bandwidths of Raman features of solid samples are also generally narrower than those of related IR bands, and therefore multiple components in sample mixtures are easier to identify using Raman spectroscopy. Absorbed or structurally incorporated water, which is often found with archaeological samples, and ambient atmospheric gases such as CO_2 are strong absorbers of IR radiation and therefore present severe instrumental and sample preparation problems for that technique. However, the visible photons in Raman spectroscopy are neither absorbed nor strongly Raman scattered by water, air, or glass, making sample analyses much easier and even allowing glass-framed objects or ones in a transparent medium to be analysed without disassembly [23,49]. The shorter wavelength of visible in comparison to IR photons allows diffraction-limited analyses of particles c. 1 μm across, providing an order of magnitude improvement in spatial resolution for Raman in comparison to conventional IR microscopy.

Powder XRD, another often utilised and superbly specific technique for identifying compounds based on their atomic spacing, is only suitable for highly crystalline samples and is limited typically to the analysis of ex situ samples, normally scrapings of material from the surface of the artefact. By comparison, Raman microscopy can be used successfully to identify even amorphous materials, including waxes and resins, and in situ on large, non-uniformly shaped objects such as statuary and codices. X-ray fluorescence (XRF) has also been widely used to suggest mineral identifications based on elemental profiles, but it cannot detect elements lighter than silicon without the benefit of an evacuated sample chamber, nor can it differentiate between samples with identical or even similar elemental composition. Polarised light microscopy, perhaps the most utilised technique for identifying inorganic crystalline compounds, requires a highly skilled operator, and even then often fails to yield conclusive—or, occasionally, accurate [18]—results on many of the important materials in archaeology and art, especially those that are organic or amorphous.

Other popular attributes of the Raman microscope are its small size and transportability. These salutary developments are allowing more extensive collaboration between academic research groups and museums, some of which remain hesitant to loan precious materials for analysis in the laboratory. The authors have on numerous occasions disassembled, packaged, shipped, and reassembled their research-grade Raman microscope in order to work on-site at London museums and libraries on objects either too large or too valuable to be brought to the laboratory [17–20,28,39,97,130]. On-site work in French museums [119] and an Italian palace [111] using transportable instrumentation has also been reported. The trend toward portability and increasingly rugged design in commercial instruments suggests that Raman microscopy is likely to expand into field-based applications in conservation, archaeology, and geology in the near future, although a truly portable field accessory capable of micrometre spatial resolution has yet to be developed. Small Raman instruments that fit in a backpack and that utilise a fibre optic probe accessory are currently offered by Ocean Optics [38] and Digilab [92], although the constraints of their portable design greatly diminish their sensitivity, spectral resolution ($\sim 15\,cm^{-1}$), and spatial resolution (several mm).

3. Applications in archaeometry

The following sections review the applications of Raman and FT-Raman microscopy to the analysis of archaeological materials. Earlier reviews have appeared as book chapters [27,29], but these works have a limited

coverage and do not provide specific commentary on the applications or their impact on archaeological research. In this review, every effort has been made to cover all research articles in English from those peer reviewed journals that are widely available. Aside from cataloguing the applications, an attempt is also made to critique the work scientifically, to seek outside comments when appropriate, and to highlight the historical and archaeological importance of the research. Because archaeometry is an artefact driven science, and one commonly confronted with extremely heterogeneous materials, the research articles are grouped based on the type of artefact being investigated, rather than by the chemical nature of the material, i.e. inorganic or organic. Raman analyses of historical textiles, illuminated manuscripts, fine art, polychrome statuary, decorative architecture, fresco, wall paintings, and related conservation and authentication studies have already been treated by the authors in an earlier review for conservation scientists and art historians [128].

3.1. Rock art and tomb paintings

Drawings in rock shelters and caves represent perhaps the earliest recorded artistic endeavours of prehistoric man. The technical analysis of these paintings seeks to answer questions regarding the availability and utilisation of mineral pigments and binding media in prehistory, the discrimination between anthropogenic and naturally occurring decorative patterns as well as modern graffiti, the chemical–chronological variations among different sites and different art types (religious, ceremonial, historical), and the geological, biological, and anthropogenic deterioration of the artwork. Naturally, the inaccessibility of many prehistoric caves is problematic for the in situ use of Raman microscopy, and so to date, all of the analyses of rock art pigments have been conducted on spallated microsamples. As battery-operated, portable instruments with remote sensors become available, their application to the in situ identification of pigments in rock art will certainly gain importance.

This area of research has naturally attracted the interest of geologists and geoarchaeologists. These specialists have voiced new concerns over confusion arising from the use of vague mineralogical terminology by archaeologists and chemical spectroscopists, e.g. 'ochre' or 'chalk' when a specific species is intended [122]. Such a warning is warranted since the identification of precise mineralogical species can be important in provenience and ancient technology studies, while inaccurate reporting is only likely to be repeated and lead to confusion in geoarchaeological research. It is expected that these problems will abate as more communication occurs between geologists, archaeologists and spectroscopists and as more extensive and reliable Raman spectral databases of mineral species and phases become available. Examples of the distinctions that are possible in the analysis of mineral artefacts and their inclusions are shown in Fig. 4. The figure includes comparative Raman and FT-Raman spectra of microscopic samples of (a) the rutile and anatase forms of TiO_2, (b) the richly coloured basic copper carbonates green malachite ($CuCO_3{\cdot}Cu(OH)_2$) and blue azurite ($2CuCO_3{\cdot}Cu(OH)_2$), (c) gypsum ($CaSO_4{\cdot}2H_2O$) and anhydrite ($CaSO_4$), (d) the common minerals calcite (trigonal $CaCO_3$) and α-quartz (trigonal SiO_2) and (e) synthetic examples of the ferruginous minerals yellow goethite (α-FeOOH) and red haematite (α-Fe_2O_3).

Capitalising on the molecular specificity of Raman microscopy, researchers have identified pigment samples from three prehistoric caves in the Quercy District of France as containing haematite, carbon black, a manganese oxide/hydroxide material, a 'disordered goethite', calcite, α-quartz, and rutile [122]. The importance of taking samples from the local environment was shown in that the identification of calcite, quartz, and rutile was attributed to their geological presence in the cave, and an incorrect attribution to anthropogenic origin was avoided. An unusual orange–brown mineral phase was found in the red haematite pigment, in some black painted areas, and also dispersed on the cave walls in the vicinity of painted regions. The Raman spectrum obtained from this material was similar to those of both haematite and goethite, but not to that of a mere combination of the two. This 'disordered' goethite was described as an intermediate phase in the natural transformation between haematite and goethite, although the direction of that transformation could not be specified. The intentional thermal transformation of yellow goethite into red haematite by ancient artists is also known and has been characterised by Raman spectroscopy [79].

The manganese material being used as a black pigment along with carbon black could not be further distinguished, although its vibrational spectrum is described as being similar to that collected from samples of the rare mineral bixbyite (cubic Mn_2O_3). The identification of this same mineral, as well as other manganese oxide phases, has been cautiously put forward by other researchers analysing black pigments from Eritrean caves [152]. The unlikely presence of natural bixbyite suggests that, if its presence could be confirmed, it might have arisen from the intentional calcination of another more common manganese mineral by ancient artists. However, manganese mineral phases are notoriously difficult to analyse by Raman microscopy due to their extreme sensitivity to laser-induced heating. Both research groups warn that the laser beam itself may have induced the formation of this unusual material, despite steps having been taken to reduce the thermal load on the samples, either by covering them with a water droplet or by using minimal laser power.

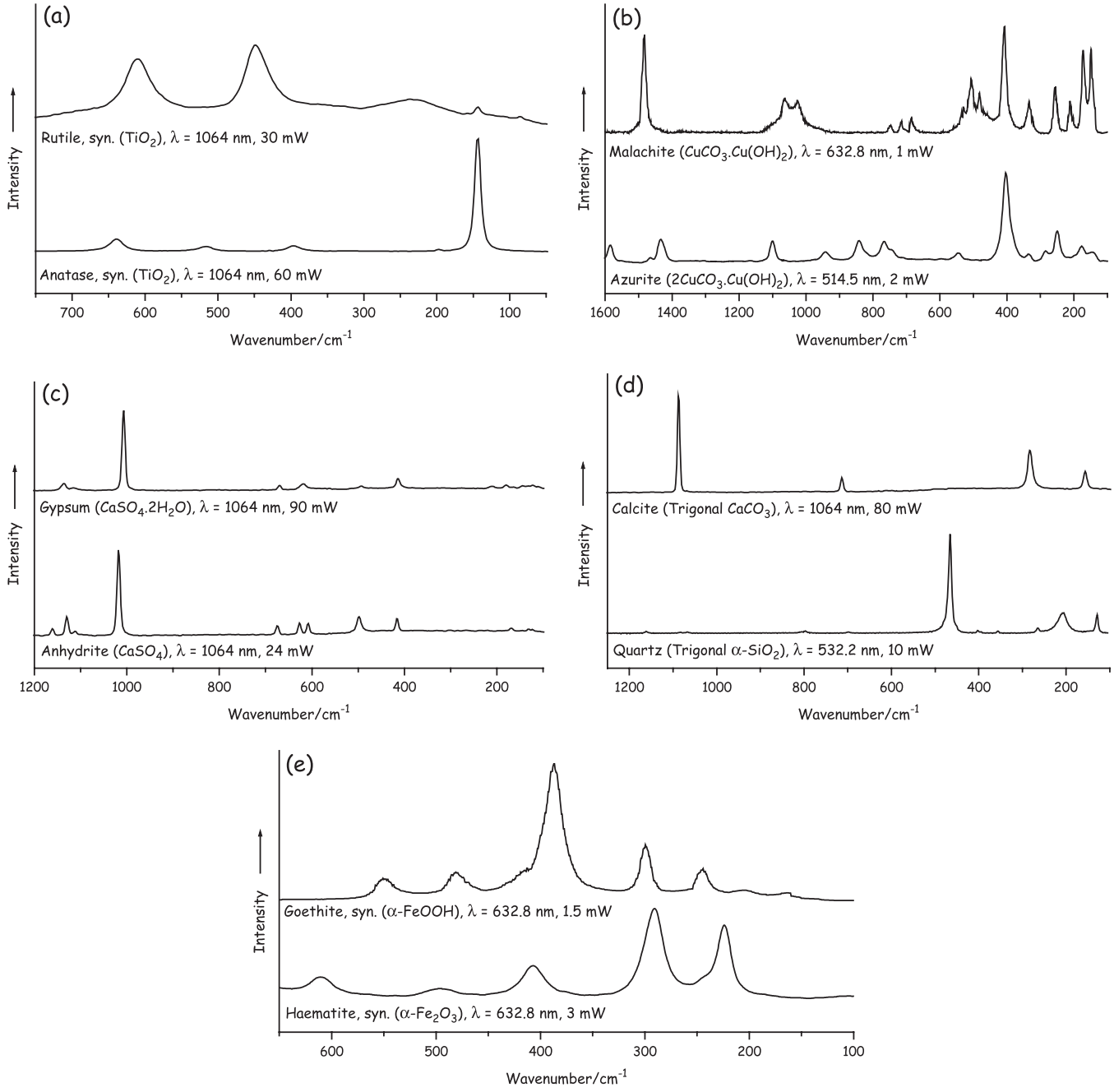

Fig. 4. Raman and FT-Raman spectra of (a) synthetic rutile and anatase TiO_2 (b) malachite ($CuCO_3{\cdot}Cu(OH)_2$) and azurite ($2CuCO_3{\cdot}Cu(OH)_2$), (c) gypsum ($CaSO_4{\cdot}2H_2O$) and anhydrite ($CaSO_4$), (d) calcite (trigonal $CaCO_3$) and α-quartz (trigonal SiO_2) and (e) synthetic goethite (α-FeOOH) and haematite (α-Fe_2O_3).

Other investigations of related rock art pigments support the above conclusions regarding laser transformations of manganese minerals. In a recent report on the 'Black Frieze' of Pech Merle, also located in the Quercy District, barium-bearing manganese minerals such as romanechite ($BaMn_9O_{16}(OH)_4$) and hollandite ($BaMn_8O_{16}$) were identified by both XRD and Raman spectroscopy as black pigments used in pictographs, although only a related manganese mineral 'wad' ($Al_5Mn_{13}O_{28}{\cdot}8H_2O$) was known to be available locally [90]. Experiments with this material showed that heating it to moderate temperatures (120 °C) generated hollandite crystals, suggesting that the prehistoric artist had calcined naturally occurring manganese minerals, possibly to facilitate their preparation as a powdered pigment. Importantly, those authors warn that the Raman spectrum of bixbyite could often be detected despite a lack of XRD data to support its presence; this

suggests that bixbyite can easily be generated by laser-induced degradation of the aforementioned Ba–Mn minerals, which now must be considered to be candidates for the unidentified black mineral discovered by Smith et al. [122]. Such an observation serves as a caveat that the identification of manganese minerals by Raman microscopy needs to be confirmed by XRD at this time. The laser intensity thresholds and optimum experimental conditions for the non-destructive identification of such minerals by Raman microscopy have yet to be established.

Transparent accretions found above and below prehistoric pictographs at numerous cave sites in the southwestern United States were investigated by FT-Raman microscopy to identify the nature of the layers [53,116]. The presence of whewellite ($CaC_2O_4{\cdot}H_2O$) was confirmed and its occurrence was attributed to biological activity of lichens [115,116] as indicated previously for deteriorating wall paintings and ecclesiastical architecture [51]. The red and black pigments used in the pictographs were identified as red ochre (Fe_2O_3 + clays) and an unspecified MnO_2 mineral, respectively [53]. The identification of the latter is professed to be the first published vibrational spectrum of MnO_2, although in fact a detailed Raman analysis of manganese oxides used in electrochemistry was performed well beforehand [3]. The identification of MnO_2 in the pictographs is based on a single band at 620 cm^{-1}, which does not match the Raman spectrum of any of the manganese dioxide phases studied in the earlier electrochemical report or in a more recent spectral library of ochres and umbers [8]. Laser-induced degradations of ramsdellite (orthorhombic MnO_2), pyrolusite (tetragonal β-MnO_2), hausmannite (Mn_3O_4) and bixbyite are all known to generate a species of unknown composition which shows a single band at ~633 cm^{-1} [3]. It is possible that the pictograph material with a feature at 620 cm^{-1} is a similar high temperature phase generated through the use of an overly intense NIR beam, the variability in wavenumber being due to variations in composition due to local heating by the laser beam. Although the authors are likely to be correct in their attribution of the pigment under study to a manganese mineral [53], the exact nature of the latter remains uncertain.

An unidentified organic component, indicated by strong aliphatic carbon bands in the manganese pigment, was also found by FT-Raman spectroscopy [53,116]. Subsequent DNA profiling purportedly showed that the material was bison or deer bone marrow, suggesting a ritual additive to the paint [74]. However, a recent attempt to replicate the ancient DNA extraction failed and raised questions regarding the possibility of modern contamination in the earlier work [105], a constant concern when dealing with small quantities of highly degraded ancient DNA. Despite this setback, the success of Raman microscopy in identifying organic remnants in some pigments could be exploited as a rapid means of selecting those pigment samples most likely to give meaningful radiocarbon dates for establishing a chronology of cave art.

Raman spectroscopic investigations of parietal artwork from prehistoric cave shelters in the New World, e.g. the Big Bend site in Texas [54,74] and Catamarca Cave in Argentina [74], have also appeared. The paintings at the former site were again revealed to contain MnO_2 as a black pigment, but this time the pyrolusite structure was confirmed by XRD. However, the Raman bands reported at 620 and 670 cm^{-1} again do not match those indicated previously in the literature [3,8], suggesting potential photo-degradation of this sensitive mineral. Occurrences of haematite in association with whewellite were discovered and attributed to natural discolouration arising from leaching of the surrounding stone by fungal hyphae and lichens rather than from the application of a red pigment. The Argentinean site is distinguished by white paintings on a dark metamorphic rock for which the white pigment was shown by Raman spectroscopy to be a mixture of gypsum and calcite on a limewash ($Ca(OH)_2$) preparation.

The palette available for decorating parietal art in the historical period is richer than that in prehistoric times. The application of Raman microscopy to ancient ecclesiastical and secular frescos has already been reviewed [51,128], but the application of decorative features to historical rock-cut tombs has not. Smith and Barbet [121] have examined mortuary artwork from a Roman tomb in Crimea and have identified a number of interesting pigments, viz. minium and Egyptian blue, along with carbon black. This identification of minium is perhaps the first recorded use of this colourant, c. 1st century A.D., although it is a common fresco pigment in later periods. A pale blue pigment from a 6th century A.D. grave in Hebei, China, believed to be that of Emperor Goa Yang of the Dongwei Beiqi Dynasty, was identified by Raman microscopy as calcite, a normally white mineral pigment [154]. After further investigation by XRF, it was found to contain significant concentrations of Mn and Fe, which are presumably the sources of the unusual blue colour. The Raman bands at 155 and 281 cm^{-1} were noticed to be exceptionally broad in comparison with those in reference spectra of the pure white mineral. The relevant modes are related to molecular vibrations involving the cation, and would be expected to be perturbed if the smaller metal ions previously mentioned periodically replaced Ca^{2+} in the lattice. The formula for this unusual mineral pigment was postulated to be $Ca_{1-x}(Mn, Mg, Fe)_xCO_3$. Cinnabar (HgS), goethite, and carbon were likewise positively identified, while an unusual combination of lead sulfate and lead monoxide was identified as a yellow colourant in a later tomb in Shoanxi Province [140].

3.2. Ceramics and glazes

Glaze, pigment, and fabric analysis of ceramics can be undertaken for the purposes of classifying artefact types, understanding developing pyrotechnologies, and revealing ancient trade routes or sources of raw materials. Raman microscopy has been used to categorise visually similar red-painted ceramics from southern Italy based on the red pigment used in their decorations. Raman and XRD analysis of the red paint on medieval Ramina–manganese–red (RMR) style ceramics identified the red colourant as iron(III) oxide [33], which matched archaeological expectations. However, the analysis of a larger collection of RMR sherds from three sites using X-ray photoelectron spectroscopy (XPS), scanning electron microscopy (SEM), and Raman microscopy showed that the different production centres could be distinguished on the basis of the different red pigments or pigment mixtures used [22]. The presence of pure haematite, pure litharge, or a mixture of haematite and litharge was found to relate a ceramic consistently to one of the three production sites. In addition to the surprising indications of craft inhomogeneity among these relatively close Italian locations, the results show that pigment analysis can be used to provide provenience for RMR ceramics when discovered without contextual data.

Similar work on fragments of an unusual blue and black glazed, low quality medieval ceramic from the same area showed that the blue background was afforded by lapis lazuli (lazurite, $Na_8[Al_6Si_6O_{24}]S_n^-$) and not a cobalt-based pigment as suspected [32,34]. However, the black pigment, found by XRD to be MnO_2, could not be positively identified by Raman microscopy at that time. This evidence for the use of lapis lazuli in ceramic production in the mid-13th century is noteworthy as this is the first identification of the highly prized mineral in a ceramic glaze, and it is surprising in this case that it was used on a low quality, local imitation proto-majolica ware. Also, this occurrence of lapis lazuli is a relatively early appearance of the mineral as a pigment in Italian art altogether. The concurrent use of lapis as a pigment in Persian ceramics has now been verified through the identification by Raman microscopy of this pigment in a 13th century Iranian ewer [41]. Mention of a *lâjvard*, or lapis lazuli, ceramic glaze in a 14th century Persian alchemical text was previously thought to indicate an imitation material meant to approximate the rich blue colour rather than one composed of genuine lazurite. The identification of lazurite in this pyrotechnology sets an upper limit for the firing temperature for the glazes at ~1000 °C, the decomposition temperature of the blue pigment.

Unglazed, painted pottery produced 5000 years ago in Henan, China was analysed by Raman microscopy and found to have been painted with bauxite (a rock containing, for instance, $Al_2O_3{\cdot}2H_2O$) for white decoration and magnetite (Fe_3O_4) for black [153]. The identification of bauxite as a locally available white material used in ceramic decoration is unusual in that sulfates, carbonates, and kaolin were normally used for this colour. Furthermore, the wavenumber of the principal spectral feature of magnetite in reference samples was found to red-shift, broaden, and decrease in intensity as the particle size was reduced. In these sherds, the magnetite particles were estimated from their Raman spectra to be in the range of 25–60 nm across, and this estimate was confirmed by XRD and transmission electron microscopy (TEM) measurements. The variation within this range was found to impart subtle changes to the colour of the pottery, perhaps capitalised on by the ancient artists. Such small particle sizes must have necessitated a rigorous preparation procedure for the pigment, although how the nano-particulates were prepared is apparently unknown. Unfortunately, no information was given regarding the spectral changes that might be expected as a result of the larger thermal load experienced by the increasingly smaller particles due to laser heating [80]. White pottery of a similar age from Xishan, China was found by Raman microscopy to be coated with anatase [155]. The intentional use of this material as an ancient pigment has not been documented previously to the authors' knowledge; its first use in fine art came only after synthetic procedures were developed in c. 1920 for producing a pure and therefore brilliant white pigment. The presence of this pigment signals a relatively low firing temperature following its application since anatase readily converts to the rutile structure at temperatures between 800 and 1000 °C. Red and black sherds from the same site were shown to be coloured by varying the quantities of red haematite and black magnetite. Two possibilities were identified for the production of these pots: either different raw materials were used to produce the ceramic colouring, or a single component, yellow/brown ochre or perhaps haematite, was used to coat the pots and different sintering temperatures and kiln atmospheres used to achieve the final colour. Under reducing kiln atmospheres, the ochre converts to haematite at temperatures up to c. 800 °C, and the latter to magnetite at 950–1250 °C.

Raman microscopy has recently been used to identify the black pigments on Ancestral Puebloan ceramics from Wallace Ruin, Colorado. A sherd from this style of pottery is shown in the inset of Fig. 5 [142]. Raman spectra similar to that shown above the photograph were recorded from the black areas of this sherd. Previous SEM–EDS analysis had revealed the presence of iron in the paint, but the specific phase of ferruginous mineral could not be identified [132]. The Raman band at 672 cm^{-1} is the principal feature of magnetite [80], thus confirming the presence of that iron oxide in the

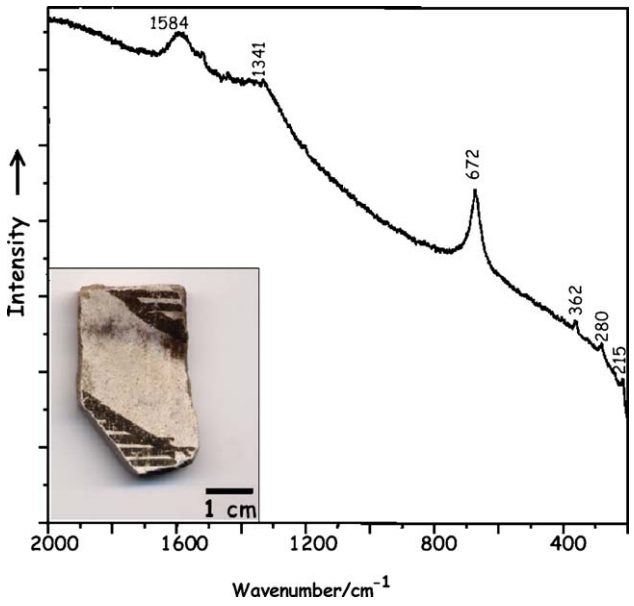

Fig. 5. Raman spectrum of the black paint on an Ancestral Puebloan black-on-white sherd (shown in inset) from Wallace Ruin, Colorado having Raman bands assigned to carbon black (1584 and 1341 cm^{-1}) and magnetite (principal band at 672 cm^{-1}).

paint sample. The lower wavenumber features could not be assigned based on available spectral databases, but the features observed at 1584 and 1341 cm^{-1} were identified as the characteristic Raman bands of carbon black [1], indicating that in this instance the black paint is a mixture. The analysis of other sherds revealed that a purely carbonaceous pigment—with no evidence of a mineral additive—was used to achieve their dark matte decoration. The use of charred animal bones, i.e. bone black, could be ruled out owing to the absence of Raman bands due to phosphate, which would otherwise have been observed at ~961 cm^{-1} [1]. The precise identification of these pigments is important for understanding the technology and use of raw materials in the production of these pots as well as in determining typologies, chronologies, and geographical extent of these ceramics [132]. Of the many techniques applied to the analysis of these paints [131–133,142], only Raman microscopy was able to detect the carbonaceous component and simultaneously identify the specific mineral phases in pigment mixtures. Moreover, the analyses were performed rapidly and non-destructively.

Pigment or fabric characterisation in ceramics can be problematic when the Raman analysis is performed through a vitreous glaze layer. This problem has been ascribed to either defocusing of the laser excitation upon passing through the glassy material [32,34], which itself can act as a lens, or to intense fluorescence generated by organics that have permeated into the porous glaze surface after years of burial [37,101]. A recent FT-Raman analysis of blue pigment particles performed through the glaze on pantiles from Bottesford, England has successfully identified azurite as the colourant [16]. The success of this study, despite an intervening vitreous layer, is attributed to the thinness of the glaze and the use of NIR radiation for which photon dispersion should be less significant and fluorescence not normally a problem. The identification of azurite as the pigment indicates a low-firing production technique since this-carbonate mineral decomposes to black tenorite (CuO) at ~300 °C. The further identifications of carbon, MnO_2, α-quartz, and red ochre are attributed to raw materials added to darken the colour of the glaze in the case of the first two and as a part of the ceramic substrate in the case of the last two. Here, the identification of MnO_2 is based on the presence of a weak, broad band at 645 cm^{-1}, a result which is in disagreement with previous band assignments for this pigment by the same authors [53,54,74]. Indications of organic constituents in the form of aliphatic bands in the FT-Raman spectra of the pantile glaze are suggested as evidence that some binder was employed in adhering the glaze to the tile. It is conceivable that this component might have survived a very low temperature firing process, but it is also possible that the organic constituent originated post-manufacture from the same gradual absorption processes that impart fluorescence to other glazed items exposed to the elements and groundwater.

Raman analysis of porcelain and celadon glazes and bodies with visible excitation has surprisingly not been hindered significantly by fluorescence from the vitreous layer [44–46,101,102]. This has been attributed to a low porosity of the porcelain glazes and therefore limited incorporation of fluorescent organic materials, as well as to the exclusion of spurious fluorescence through the use of a confocal optical geometry. The analysis of the glaze and body of 13th–16th century Vietnamese ceramics allowed various production sites to be classified as manufacturing either proto-porcelain, true porcelain, or faience [46,101]. This determination was based partially on the comparison of relative amounts of crystalline quartz remaining in the body as demonstrated by bulk analysis Raman spectroscopy. The presence of mullite ($3Al_2O_3{\cdot}2SiO_2$) in the ceramic body confirms a high temperature firing (1200 °C) of the kaolin ($Si_2O_5(OH)Al_2(OH)_3$) used in its production, while anatase inclusions discovered in the glaze by Raman microscopy indicate a later application of the glaze in a second firing at lower temperature (v. supra). These results were confirmed by differential thermal analysis (DTA) curves obtained from the ceramic fragments. Comparison of the glazes from ancient Vietnamese porcelains of different temporal and geographical regions and from modern imitations showed that the glaze composition could be inferred from its Raman spectrum and that modern imitation porcelain glazes, which are shown to contain α-wollastonite ($CaSiO_3$), are easily distinguishable from

authentic ancient wares that do not possess this mineral phase.

This research has since been extended to the analysis of the interface area between the glaze and the ceramic body where a white layer is observed visually [102]. Confocal Raman microscopy through the vitreous outer surface has identified the interface layer as a mixture of mullite, rutile, and α-quartz, with the Raman features of the last material bearing indications of the tensile stresses imposed on the interface by differential cooling of the ceramic body and outermost glaze. Analyses of ancient and modern European porcelain has revealed that Raman spectra can be used to distinguish easily between soft-paste and hard-paste porcelains based on the presence of β-wollastonite and/or tricalcium phosphate (β-$Ca_3(PO_4)_2$) in the former and mullite in the latter [44]. The glaze composition can be inferred from a deconvolution component analysis of the scattering envelope due to the O–Si–O modes. Small changes in the relative intensities of component bands are due to characteristic interactions of the glaze fluxing agents with the vitreous phase. The identification of pigments and dissolved colouring ions employed from antiquity to the modern era for elegant glazes and enamels has been reported, and a Raman spectral library has been constructed from these results [43].

Raman microscopy has also been used to perform spectrographic petrography of mineral inclusions in the fabric of unprepared ceramic sherds [150,151]. Petrography is used routinely in the analysis of archaeological ceramics to identify and quantify the mineral component of the clay fabric in order to suggest a provenience for the artefact or to investigate its method of manufacture. The analysis is often performed visually by PLM using laboriously prepared translucent thin sections. Alternatively, a purely descriptive assessment of the shapes, colours, sizes, and numbers of the various inclusions can be made by incident light microscopy. The sherds can then be grouped based on like assemblages of inclusions. In their analyses of unprepared sherds of 3rd–2nd century B.C. domestic wares collected from the Agora in Athens, Wopenka et al. [150] have utilised the chemical specificity of the Raman technique to identify the various types of inclusion and then semi-quantify those types based on a visual tally of the different forms. The use of spectral libraries simplifies the application of the technique so that little operator training is required; this, combined with the use of unprepared sherds, makes the process of identification extremely rapid. Quartz, rutile, anatase, calcite, haematite, anhydrite, albite ($NaAlSi_3O_8$), epidote ($Ca_2Fe^{III}Al_2O(Si_2O_7)(SiO_4)(OH)$), and apatite ($Ca_5(PO_4)_3(F,OH,Cl)$) were identified as either course temper added to the pottery or secondary minerals formed by the firing of the clay matrix. Analysis of the fired clay itself gave only weak Raman spectra that were not interpreted by the authors due to the dearth of related Raman research on dehydrated ceramic clays. This deficit suggests a further area of archaeometric research where valuable information might be gained. Clearly, Raman microscopy can be a useful addition to the standard techniques of SEM, XRD, and PLM employed by ceramicists.

3.3. Glass and faience

Few early reports of the Raman analysis of glass artefacts exist, although this situation is now changing with increasing interest in glass technology and raw materials and concomitant improvements in the Raman instruments used to investigate them [9,11,12,124]. The early hesitation to work with glass artefacts is attributable to the weak Raman scattering of vitreous silica, as well as to the tendency of the latter to fluoresce strongly as a result of burial environments or artefact handling. However, analysts examining 18th–20th century artistic glasses ingeniously turned the normally nettlesome fluorescence of glass objects to their advantage in developing a dating scheme which has attracted surprisingly little attention [5]. The ratio of the intensity of the 1080 cm^{-1} Raman band of vitreous silica to that of a fluorescence band centred at $\sim$2000 cm^{-1} provides an analytical variable that is correlated with the age of the artefact; the fluorescence increases with the age of the glass. Over the 200 years spanned by the artefacts examined, a chronological calibration curve shows remarkably good sensitivity and linearity, suggesting that dating to better than a decade is easily achievable. This scheme has only been tested on relatively young, clear, and compositionally similar glasses in a pristine state of preservation, and no data are available that indicate whether the technique could be extended to ancient glassware recovered by excavation.

Excavated glasses represent a significant problem in terms of analysis in that they are often friable, partially degraded, and impregnated with fluorescent components and groundwater salts. Nevertheless, inclusions in the weathering crusts of potash glasses recovered from various excavations were identified by Raman microscopy as containing calcium phosphate species [48]. No such inclusions were found for soda-lime glasses of comparable age. This information would seem to corroborate the practical experience of archaeologists, who often find that natural groundwaters penetrate the outer surface of northern European glasses (typically potash-based) and leach alkaline and alkaline earth oxides, causing the weathering layers, crystal growth, and ultimately the disintegration of the glass. Soda-lime glasses, common for instance in the ancient Middle East, are known to be much more robust, and often survive millennia in periodically soaked burial environments. Surprisingly, a second, independent study assessing the

weathering of Italian medieval glass revealed that the soda-lime glasses that were examined had heavily weathered surfaces while the single potash glass being studied was relatively pristine [6]. Raman spectra of microscopic, flat crystal aggregates found in the weathered layers of the soda-lime glass were identified as complex carbonates, calcite cores radiating vaterite (hexagonal $CaCO_3$) needles; the vaterite was slowly transforming to the more thermodynamically stable calcite. These two, very different, conclusions regarding archaeological glass degradation suggest that glass weathering is extremely complex and, not surprisingly, may be highly specific to the burial environment. Unfortunately, no analysis of the soil chemistry of the excavation site was undertaken in these studies.

The weathering on 6th–5th century B.C. opaque red glass enamel from ancient Nimrud has also been investigated [149]. Cuprite (Cu_2O) was identified as the red colourant in the glass, and colloidal copper was also observed visually. The presence of the latter is probably a result of excessive reduction of the oxide by charcoal used to maintain the cuprous state of the opacifier during the annealing of the glass. Litharge was also shown to be present, and is likely to have assisted in dissolving the opacifier in the molten glass. Portions of the glass rim were discoloured green and warranted special attention. Elemental profiling of the red and green areas showed no noticeable differences in composition; however, Raman spectra of the green portions revealed a complex mixture of weathering products including malachite, cerussite ($PbCO_3$), gypsum, and calcite. For yellow Anglo-Saxon glass beads from the 6th century A.D., lead tin yellow type II was identified as the opacifier, also used in combination with litharge. Ancient Phoenician beads, tessarae, and jewellery composed of clear and coloured glass have also been examined in order to discover the technology involved in their manufacture: leaded glass could be distinguished from soda-lime glass based on the characteristic shape of the Raman band assigned to the silicate matrix, cassiterite (SnO_2) was found to be used as a fluxing agent or opacifier in some instances, and pigments, mineral inclusions, and imitation materials were identified [42]. These results were confirmed by SEM–EDX and XRF. In surface-painted medieval and Victorian English ecclesiastical window glasses, haematite was found to have been used without additives as the pigment for producing dark red–brown geometrical and clover leaf decorations [76].

Pigments used in the decoration of faience, a silica frit, have also attracted the attention of Raman spectroscopists. The examination of Egyptian polychrome faience from El-Amarna identified Naples yellow ($Pb_2Sb_2O_7$) and red ochre as the yellow and red colourants, respectively, but failed to identify the blue, green, and white pigments in other sherds [37]. The two positive identifications are consistent with the use of earth pigments in 18th Dynasty Egypt (1570–1293 B.C.) and the availability of an antimony oxide for synthesising Naples yellow.

3.4. Lithics

Raman microscopy has become an important tool in paleontology and earth sciences [107,123,136]. Smith et al. have shown the advantages of the Raman microscope in the analysis of several types of mineral artefact including Celtic vitrified forts [127], Roman intaglios [126], and Mesoamerican 'greenstone' axes [125], and the classification of mineralogical samples in museum collections [119]. The application of the technique to unprepared samples was important in each of these studies due to the high value, both monetarily and historically, of the materials.

The identification of the rare, high temperature silicate phase α-cristobalite (tetragonal SiO_2) in samples of a fused Celtic fort has allowed an estimate of the temperatures achieved in the vitrification process to be made [127]. This mineral is normally formed upon the cooling of β-cristobalite, itself requiring a temperature of 1470 °C to be formed from α-quartz, well above that originally thought possible in antiquity for fusing such massive objects. This discovery necessitates a reconsideration of ancient pyrotechnological capabilities. It is worth noting, however, that more recent work has raised questions as to the precision, and therefore the usefulness, of α-cristobalite as a geothermometric marker in certain circumstances [109].

The analysis of three differently coloured French intaglios of the early Roman period revealed that they were all composed of chalcedony, i.e. microcrystalline α-quartz [126]. Although elemental analysis was not undertaken to determine the particular colouring ions, two of the items were further categorised as chrysoprase based on their green shades, while the metallic gray intaglio was conventionally labelled jasper. The Raman features of the previously controversial mineral phase moganite (monoclinic SiO_2) were also observed. The now recognised presence of moganite in artefacts previously classified simply as chalcedony suggests that further characteristic distinctions between the different types of silicate minerals are perhaps possible [114].

Two axeheads composed of greenstone were specifically identified by Raman microscopy as being composed of a titanite-rich ($CaTiOSiO_4$), amphibole-bearing eclogite material and a jadeite-jade ($NaAlSi_2O_6$), respectively. Importantly, this identification was performed without requiring thin sectioning of the valuable artefacts [125]. The latter axehead was obtained from outside an archaeological context, and therefore might be a modern forgery, but the former is from a pre-Columbian archaeological site on Cozumel Island. This

island lacks eclogite facies, and the axehead is the first recorded pre-Columbian eclogite artefact in the Americas. Smith and Gendron suggest likely sources for the artefact material from nearby locations, emphasising the possibility of utilising Raman microscopy for artefact provenience without destructive sampling. New information regarding the possible source of the jadeite axehead has been derived from the same authors' discovery and subsequent Raman analysis of a jadeite-jade river pebble in an area of Guatemala until now thought to be devoid of jade sources, the southern Montagua River Valley [84]. The results showed that the composition of this particular form of jade, comprising jadeite, rutile, titanite, and quartz, is unique not only within Guatemala but also worldwide. The identification of this area as a source of jadeite-jade provides a possible provenience for the raw material used to manufacture the jadeite axehead, although it does not establish it as an authentic artefact.

The Raman analysis of mineral inclusions contained in over 350 garnets from French 'cloisonné' jewellery of the 5th–7th century A.D. Merovingian period highlights another use of the technique for provenience studies [26]. The major elemental compositions of the garnets, determined by particle-induced X-ray emission (PIXE) spectroscopy, allowed them to be classified as almandine ($Fe^{II}_3Al^{III}_2(SiO_4)_3$), pyrope ($Mg^{II}_3Al^{III}_2(SiO_4)_3$), or an intermediate between those end-members. Each of the groups could be further divided into two sub-categories based on their elemental profiles. Raman analysis of the mineral inclusions in the almandine garnets confirmed the sub-classes; one group was found to contain a large collection of inclusions comprising rutile, quartz, calcite, apatite, zircon ($ZrSiO_4$), ilmenite ($FeTiO_3$), monazite ($(La,Ce,Nd)PO_4$), and graphite (hexagonal C) while the other was sparsely populated with only rutile, apatite, and monazite crystals. The pyropes were devoid of any inclusions. The elemental profiles determined by PIXE were compared to literature databases to suggest specific eastern European and Asian sources for the garnets. Further information on typical mineral inclusions in garnets from the above locales—particularly Raman-based information from either the extant geology literature or newly established—is needed to substantiate the suggestions as to the sources of these gemstones.

The Raman technique has also been used extensively in gemology to detect faked, imitation, and artificially improved jewels, as well as to identify faux 'gemstones' in historical items [98,118]. An analysis of two gem-encrusted ecclesiastical pieces from the Basel Cathedral, the Reliquary Cross and the Dorothy Monstrance, revealed a large number of coloured glass 'stones' as well as doublets, i.e. two joined quartz crystals with a painted interstitial layer [91]. Surprisingly, the doublets in the latter artefact were colourless, suggesting that a fugitive paint had been used in the cement layers. Twelve gemstones set into the cover of an elaborately decorated leather-bound manuscript, the Tours Gospel, "Evangelia Quatuor", held in the British Library were identified by Raman microscopy to be composed of silica, amethyst, emerald, iron garnet and sapphire [39].

Mineral collections in various French museums have been studied successfully with transportable Raman instruments utilising remote laser fibre optic probes [119]. The utility of these systems lies in the effectiveness by which large numbers of minerals may be identified rapidly without the need to disturb the artefacts, either by removal from their protective display cases or by sample preparation. The fabric and associated pigments of several large sculpted stone masks in the Musée de l'Homme in Paris were also identified using a mobile Raman system with a horizontal microscope accessory [119,120]. Fig. 6 shows the system during the analysis of the famous Aztec skull carved from a single transparent mineral crystal. The spectrum of the skull corresponded to that of α-quartz and confirmed the historical assignment of the material as 'rock crystal', although other purportedly rock crystal artefacts were in fact discovered from their Raman spectra to be composed of a different material.

These applications highlight the utility of Raman microscopy in the field of geoarchaeology as well as in the analysis of mineral artefacts. Clearly, Raman microscopy offers a compelling, non-destructive alternative to thin section petrography, XRD, and SEM analysis when the surface of the artefact is of interest or can be considered representative of the whole. However, the analysis of some mineral species, namely those that are blackbody absorbers, has not always been successful. An early article reporting the Raman analysis of jet and jet-like artefacts found that the identification of archaeologically important black minerals, viz. jet, lignite, and cannel coal, was problematic [96]. Only weak peaks due to phenyl (C_6H_5) rings were observed, and these features were identical for all samples. It must be noted, however, that this work was done prior to the advent of the highly sensitive Raman systems currently available, and several seemingly hopeless analyses of black minerals, e.g. plattnerite (PbO_2) [25], magnetite [80], and galena (PbS) [129,130], that were impossible or nearly so five years ago are now being fully realised.

3.5. Metals

Although the Raman technique is insensitive to most pure metals and alloys, it is well suited to the identification and study of corrosion and patina layers on metal artefacts as well as of the inclusions found in metal objects and slag. The analysis of Chinese bronze *yaoqianshu*, or money trees, has made use of this capability [106]. Stylistic analysis, as well as the identification by Raman microscopy of corrosion species on

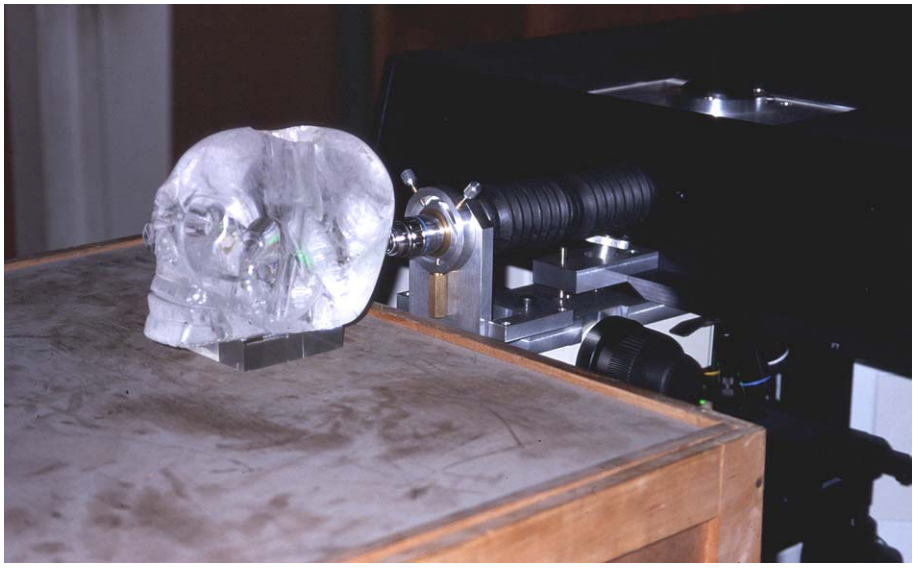

Fig. 6. Photograph of a mobile Raman microscope based on a Dilor Labram with a side-looking objective being used to analyse an Aztec 'rock crystal' skull in a storage facility at the Musée de l'Homme in Paris in 1999 (courtesy Dr. David C. Smith).

various branches of one tree, have shown that the statue is actually composed from parts of as many as five separate money trees, each having been exposed to different environmental conditions and therefore having a different host of degradation products. Notably, the examination of cross-sections of the exposed surface detected the presence of sulfate and sulfide corrosion products, suggesting that the money trees had been either exposed to modern air pollution or buried in anaerobic soils with sulfate-reducing bacteria. Alternating corrosion layers have also hinted at cyclically varying burial conditions for some branches of the money tree. The analysis further identified a number of modern pigments, e.g. phthalocyanine blue ($CuC_{32}H_{16}N_8$), that had been applied to repaired sections of the money tree in more recent times in order to simulate a realistic patina layer.

A pale blue corrosion material identified on numerous copper alloy artefacts in several museums has been identified using Raman microscopy and other techniques as a product of its display environment rather than as a natural patina [134]. The complex salt, a copper–sodium–formate–acetate material of unspecified stoichiometry, probably originated from a coincidental presence of cleaning compounds such as sodium sesquicarbonate and formic and acetic acid vapours emanating from the wooden display case in which the bronze statue was housed. Curiously, the product was not seen to occur on repairs to the statue, which was made of brass, an alloy of copper and zinc. The authors report that Zn/Cu catalysts are used in the industrial process of forming methanol from formic acid, and therefore the protection afforded to the brass may lie in its ability to eliminate the formic acid vapour before it can react to form the pale blue corrosion product.

The utility of Raman microscopy in the identification of corrosion layers on ancient coins composed of various metals and alloys has been demonstrated and shown to be well adapted to the non-destructive analysis of these small finds [10]. The identification of the assemblage of corrosion products on a particular coin was found to reveal very approximately the alloying composition of the coin; this could however be largely affected by the preferential corrosion of some elements relative to others. As a proof-of-concept application, this research shows the potential of the technique for classifying coin composition, suggesting previous burial environments based on the profile of corrosion products, and informing conservators as to the seriousness of a coin's past, and possibly future, deterioration. The same authors have recently completed a catalogue of Raman spectra of minerals pertinent to metal corrosion [12]. Another numismatic study involving Raman microscopy has investigated 19th century metallurgical processes. Inclusions of magnetite, iron-deficient magnetite, and haematite in a 1837 Russian coin made of platinum were shown to have formed by phase separation upon oxidation of the iron alloyed with the platinum [141].

The surfaces of Chinese *heiqigu*, or black bronze mirrors, were examined using Raman spectroscopy in order to investigate the surface coating responsible for their anti-corrosion property [139]. In this instance, the sample was analysed by scraping the surface of one artefact and introducing the material to the laser beam in a glass capillary. Although invasive, the analysis showed that the anti-corrosive black coating was nanoparticulate SnO_2, perhaps doped with atoms of Cu, Fe, Pb, and Si. The presence of this latter group of elements was indicated by complementary elemental techniques.

Other highly corroded bronze and brass artefacts have been found to be an unexpected source of two minerals, buttgenbachite ($Cu_{36}Cl_6(NO_3)_4(OH)_{62}\cdot 12H_2O$) and connellite ($Cu_{36}Cl_6(SO_4)_2(OH)_{62}\cdot 12H_2O$), which occur only rarely in nature. The Raman spectra of these two end-member minerals have been measured, opening the way for future studies of such compounds and their intermediate forms in artefact patinas [12,83]. Similarly, atacamite ($Cu_2Cl(OH)_3$) and paratacamite ($Cu[Zn,Ni,Co])_2Cl(OH)_3$), as well as the basic copper sulphates antlerite ($Cu_3SO_4(OH)_4$), brochantite ($Cu_4SO_4(OH)_6$), posnjakite ($Cu_4SO_4(OH)_6\cdot H_2O$), and langite ($Cu_4SO_4(OH)_6\cdot 2H_2O$), which often occur as patina minerals and occasionally as degradation products of copper pigments, have been characterised thoroughly by Raman microscopy [9,12,82,104].

3.6. Ancient technology and pigment synthesis studies

The characteristics of Raman microscopy that make it so well suited to the applied research mentioned above also allow it to be used to great effect for basic research in understanding ancient technologies and crafts. Aside from the reconstructions of pottery firing conditions already mentioned, this area of research has concentrated on understanding the technology used in the production of artists' colours [30,36,108]. For instance, resonance Raman spectroscopy was used to investigate the effects of synthesis conditions on the final colour and properties of a historic pink porcelain glazing pigment, a chromium-doped tin-based sphene, used at the famous French Sevres Factory [81]. The calcination temperature was found to be less important than the presence of secondary phases, pigment crystallinity, and particle size in determining the colour of the pigment.

The ancient fabrication processes of Egyptian blue and green pigments have also been investigated by Raman microscopy. The crystalline inclusions in cakes of Egyptian blue and green pigments from the New Kingdom era (1567–1085 B.C.) have been used as chemical indicators of the manufacturing processes [109]. The raw pigment cakes allow the unrefined products to be examined without any interference from artistic preparations. Raman spectra showed the blue pigment to be composed of cuprorivaïte ($CaCuSi_4O_{10}$) while the green (actually turquoise) pigment gave a Raman spectrum identical to that of β-wollastonite. Complementary SEM–EDX analysis showed that the Egyptian green contained about 2% Cu. Surprisingly, the Cu is reported to have no effect on the Raman bands of the host crystalline material. The authors hypothesise that the Raman spectra of β-wollastonite and 'cuprowollastonite' are identical, but this supposition would require additional scientific proof that the copper observed by SEM is even incorporated into the silicate mineral. Incidentally, the barium analogue of Egyptian blue, known as Han blue ($BaCuSi_2O_6$), does have a distinct Raman spectrum and has been identified by this technique on painted figurines from Chinese tombs dating back almost 1900 years ago [156].

In both the Egyptian blue and Egyptian green samples, amorphous quartz was identified along with high temperature α-cristobalite, although the latter was rare in Egyptian green samples, suggesting that the green pigment's manufacture might have involved the lower temperatures. Deep inside the amorphous matrix of both pigments, particles of CuO and SnO_2 were identified, suggesting that an overall oxidising rather than a reducing furnace was used and that bronze, a Cu–Sn alloy, served as the raw material source of copper for the pigments.

Other researchers have also examined the fabrication of Egyptian pigments including Egyptian blue. Wiedemann et al. [143] used Raman microscopy as well as DTA to study the composition of Egyptian blue from a painted bust of Nefertete as well as contemporary 'Talatats', or decorated tiles, from the disassembled temple at Karnak. The pigments were identified by Raman spectroscopy while DTA quantified the unreacted raw materials, viz. quartz and calcite, contained in the pigment. Raman analysis of the Talatat pigments also showed that the Egyptians made use of mineral sources containing potential tracer compounds like a red mixture containing huntite ($CaMg_3(CO_3)_4$) and also a pure reddish-brown pigment composed of zincobotryogen ($(Zn,Mg,Mn^{II})Fe^{III}(SO_4)_2OH\cdot 7H_2O$); without this scientific analysis, these pigments might otherwise have been thought to be common earth oxides. Laudably, these researchers also scoured natural mineral sources in North Africa in order to obtain authentic reference materials for comparison to the artefact samples.

3.7. Textiles and plant fibres

Much interest has been placed on the Raman analysis of resins and dyes commonly used in antiquity in conjunction with mordants for dying cloth [47,55,69,88,89,112,148]. Many of the dye chromophores exhibit resonance Raman effects, and therefore extremely low concentrations of these colourants are still detectable in the cloth. Less attention has been placed on the identification and study of the plant fibres themselves that are used in traditional as well as modern societies for the manufacture of textiles, baskets, and mats. However, a catalogue of Raman spectra of various natural fibres has been compiled [71], and the stage is set for further work with actual archaeological materials. Flax, jute, ramie, cotton, kapok, sisal, and coir were all included in the catalogue. A methodical protocol is suggested for identifying the fibres in ancient textiles and domestic goods, and also for determining the state of

fibre preservation. Cellulose, a component common among all the aforementioned fibres, consists of glucose monomers connected by ether (C–O–C) linkages. These linkage sites are prone to enzymatic and oxidative cleavage, and so one can estimate the condition of the archaeological fabric by monitoring the Raman bands due to the ether component relative to those of CH_2 functional groups, which are expected to form at the sites of degradation [55,58].

3.8. Resins, waxes, and organic residues

Preserved resins and waxes are rare in the archaeological record, primarily because they often succumb to predation by insects and bacteria, are easily damaged by light, heat, and humidity, and can become friable and thereby lost during interment or excavation. Although they seldom survive harsh burial environments, their occasional occurrence in the archaeological record offers an important opportunity to learn more about their sources, processing, trade, and use in crafts and routine domestic life in antiquity. Because of their tendency to incorporate or develop fluorophores that frustrate conventional Raman microscopy with visible excitation, these items have been analysed most often by FT-Raman spectroscopy. The non-invasive and non-destructive nature of the Raman technique offers an extremely important advantage over the destructive gas chromatography-mass spectrometry (GC-MS) methods commonly used to identify and study small amounts of precious ancient organic materials. The wax or resin can usually be examined using a Raman microscope without even requiring its removal from the artefact, thereby ensuring its availability for future analysis or display in museums.

Plant resins are composed of numerous components; chief among these are terpenoid and alkene polycyclic compounds such as (a) abietic acid and (b) Δ-8(9)-isopimaric acid, shown in Fig. 7. A recent study has revealed that the conjugated and aliphatic alkene bands (1500–1750 cm^{-1}) of resin sealants from Native American bottles and baskets were useful for identifying the nature and source of the material, which had previously been called generically "pine pitch" or even "bitumen", suggesting that they might be petroleum based [56]. The study distinguished between modern samples of colophony, rosin, and several species of pine resin on the basis of their Raman spectra. The artefact resins gave spectra which corresponded roughly to those of pine resins from the region of excavation; however, differences in the C=C stretching region of the spectra and those of modern reference materials hint at diagenetic changes in the archaeological material during burial. This work has since been extended to resins found on 2300-year-old Vietnamese burial jars [75]. In that study, the alkene region of the Raman spectrum was again

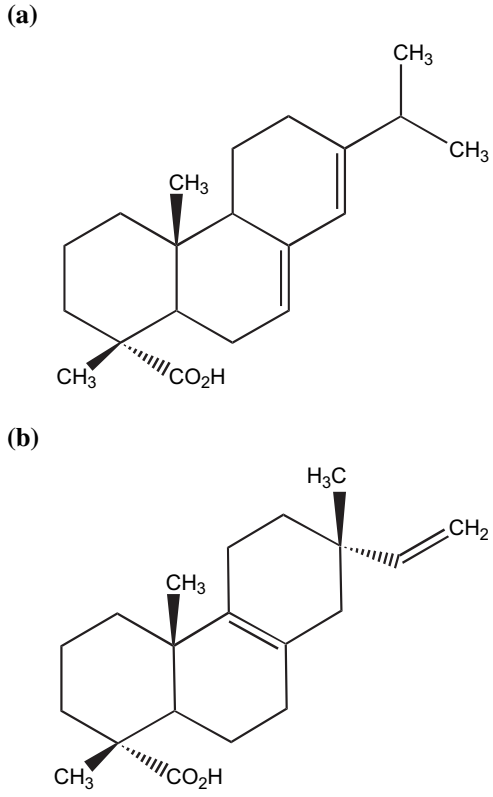

Fig. 7. Common terpenoid and alkene components of archaeological resins: (a) abietic acid and (b) Δ-8(9)-isopimaric acid. N.B. similar figures have appeared in the relevant literature [56,57,75], but both structures were drawn incorrectly [146].

used to characterise two ancient Vietnamese resins and three modern samples of indigenous resins. The ancient Asian resins were shown, not surprisingly, to be different from those on American artefacts, but unfortunately they could not be identified positively by comparison with the modern reference samples from Vietnam. Significant band broadening in the spectra from the Vietnamese artefacts is suggested as being indicative of increased degradation, perhaps due to a (presumably) more humid burial environment or to a larger component of the less stable abietic acid than is found in the American resins.

The temporal changes in archaeological resins have also been investigated by FT-Raman spectroscopy. The ratio of the intensity of the alkene (C=C) stretching band at ~1640 cm^{-1} to that of the methylene ($C=CH_2$) deformation band at 1440 cm^{-1} in fossilized resins (ambers) provides an analytical variable that relates to the age of the sample [62]. The ratio decreases as the sample matures because the alkene functional groups are depleted due to crosslinking and oxidation. In these analyses, a modern pine resin sample showed a ratio of 1.7 whereas a genuine amber sample had a value of 0.6. Although obviously ancient, the amber sample was further designated "geologically young" by the authors

because it showed no spectral features due to aromatic moieties, which are another purported component of mature amber. Since then, the maturation process of archaeological resins has been elucidated more fully using a larger set of samples that span modern to ancient specimens [147]. Fresh resin samples, sub-fossilized materials (copals), and fossilized ambers up to 130 million years old were examined, and the analyses confirmed the loss of alkene functionality with age. However, no concomitant increase in aromaticity with age was observed, raising doubt about the usefulness of that particular chemical indicator in determining resin maturity.

Another study examined geographically distinct amber samples from the Baltic, Poland, England, Northern Germany, Dominican Republic, Mexico, Kenya, East Africa, Burma and Borneo [14]. The samples were roughly dated based on their archaeological context. Disappointingly, unlike similar studies using IR spectroscopy, no clear Raman spectral features were found to be characteristic of the specific geographic regions. Moreover, the analyses showed that the temperature, water content, and pressure of the burial environment have had a significant effect on the maturation process in ambers. This discovery invalidates a strictly temporal interpretation of the dating scheme based on the alkene/methylene band ratio mentioned above. As a further impediment to dating amber fossils, the sample from Borneo was shown to be most likely composed of a triterpenoid resin rather than the more common diterpenoid abietic acid discussed so far. Although understood to be immature from its archaeological context, the sample provided an extremely low band intensity ratio, paradoxically suggesting great geological age. Considering these results, it can be surmised that the use of band intensity ratios as a dating method alone must be practiced carefully on well characterised samples and can only be expected to provide a rough estimate of age.

Although the provenience of the amber specimens could not be determined based on their Raman spectra, attempts to understand the origin of other archaeological resins have not been entirely futile. Historically, different cultures acquired "dragon's blood", a red resin valued for its decorative and antiseptic properties, from different plant species. Examples of several types of this resin from different sources have been characterised by FT-Raman spectroscopy [69]. Variability in the Raman spectra is expected depending on the types and quantities of the various red chromophores present, e.g. dracorubin, dracorhodin, dracoresinotannol, and dracoresene, as well as other volatile and non-volatile components of the plant product. The Raman spectrum of one type of dragon's blood, which was in fact not a plant resin but a gum collected from ant galls occurring on the host tree, was shown to be distinct, while the other samples, all true resins, showed more moderate spectral differences. Moreover, four samples of the same resin species collected at different locations on Socotra Island were declared also to be spectrally distinct, leading the authors to propose that sample provenience might even be deducible on a regional scale! This suggestion, however, is not yet credible owing to the limited sample population considered; only the resin from a single tree from each grove was analysed. A nearly identical study has appeared in which the identification and provenience of genuine and imitation brazilwood dyes was sought, although again, the sample population was limited to a few examples from a small number of localities, and many of these were of questionable attribution or of unknown age [52].

It is believable, however, that local environments can affect the composition of a plant resin and by extension its Raman spectrum, but whether this represents a boon or bane to archaeometric analysis is arguable. For instance, a cursory study of modern, unprovenienced samples of frankincense and myrrh, both complex resin mixtures, has shown that the two can be distinguished from each other [15,57], which is hardly unexpected since their plant sources and their major chemical components are different, e.g. myrrh has a very high gum content in addition to the triterpenoids that are common to both resins. However, the spectrum of each resin type itself changes with the climate and environment in which the plants grew, as well as the purity, season of collection, and processing of the resin. Consequently, resin pearls from the same sample lot provided somewhat different FT-Raman spectra [15]. The task of sorting out the effects of all these variables on the spectrum of a resin sample seems daunting and impracticable.

It is most probable that the utility of archaeometric analysis of organic residues by Raman microscopy will be in the non-destructive assessment of their general chemical nature, e.g. resin, gum, or wax. This is eminently possible since these broad categories of materials vary greatly in their primary chemical constituents [75,138]. The resins, as mentioned previously, contain a large terpenoid and polycyclic component (see Fig. 7), as well as various aromatic, ketone, alcohol, and carboxylate compounds. Fig. 8 provides generic structures for the major components constituting (a) gums and (b) waxes. The gums are generally polysaccharide compounds, and the waxes contain long chain hydrocarbons, fatty acids, and esters. Each of these groups bears structural features with distinct spectral signatures that allow relatively straightforward discernment. Moderate powers of discrimination have been professed for refining these groups further into individual species of resins [15,63], gums [59], and waxes [60,63]. However, in some instances, complicated chemometric techniques have been required to unmask the faint variations in the seemingly identical

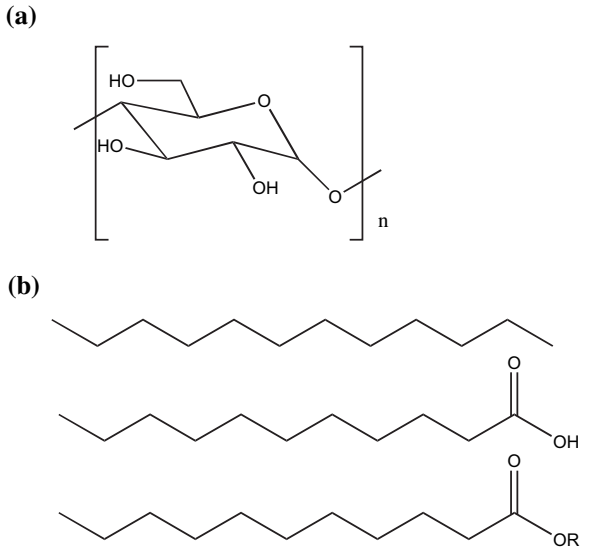

Fig. 8. Generalised molecular structures of the major components of (a) gums and (b) waxes. The generic structures are those of polysaccharides in (a) and aliphatic hydrocarbons, carboxylic acids, and esters in (b). The third category of organic residues, resins, are composed of the diterpenoids and polycycles mentioned previously plus various aromatic, ketone, alcohol, and carboxylic acid compounds.

spectra [59], and in other instances even modest degradation due to aging appears to homogenise spectral differences [15]. Only a few classes of materials show more palpable spectral diversity within the group, for example the saturated and unsaturated waxes are distinct sub-groups [60] as are the diterpenoid and triterpenoid resins [15].

Since most of the reference spectra of the organic residues are derived from single, pristine examples of each material, it is not yet known whether these spectral libraries will be useful in the specific identification of real artefacts that have undergone traditional processing, natural aging, and prolonged degradation. To date, only one instance has been reported in which an unknown historical residue was specifically identified, viz. beeswax on a 19th century historical photonegative paper [63]. This lone identification, too, seems to be in error based on a subsequent publication by one of the same authors [60]. A sharp, unexplained band in the spectrum of the artefact at $\sim 1610\,cm^{-1}$ is clearly absent from the reference spectrum of pure beeswax and from that of the paper substrate [63], but it has now been shown to exist in the reference spectra of numerous unsaturated waxes, e.g. carnuba wax [60] which, outside of further evidence, suggests that the photonegative is instead coated with one of these materials. Other tentative assignments of historical residues found on funerary objects have been put forward recently as possibly being myrrh, fronkincense, and dragon's blood, although the spectra were of poor quality and the analyses suffered from considerable fluorescence even when performed with NIR excitation lasers [77].

3.9. Biomaterials (skin, hair, teeth, bones, and ivory)

A voluminous literature exists on the Raman analysis of human and animal bioartefacts including teeth [4,78,99], mummified skin [65,72,73,85,86,144], hair [145], 'organs' [65], bone [64,72], hooves and nails [50,72,73], and ivory [13,61,66–68,117]. Because of the intrinsic or acquired fluorescence of these materials, all these projects have utilised an NIR laser and an FT-Raman spectrometer. The archaeological objectives of this type of research are diverse and include ascertaining the state of preservation of the biomaterials, determining the cause of death and post-mortem treatment of the body, resolving body art from disease or posthumous skin damage, identifying the animal species from which the biomaterials are derived and, in rare instances, using changes in the artefact's composition to specify the time lapse since death.

Regarding the last goal, i.e. that of dating, FT-Raman spectroscopy has been used to probe the organic (collagen) and inorganic (apatite) content ratio of modern and ancient teeth [4]. The loss of protein in tooth enamel can be related to the age of the bioartefact, and a calibration curve was constructed by plotting the artefact's age versus the ratio of the intensities of the CH_2 stretching band and that of phosphate. The relative loss of protein was found to be rapid during the first 1000 years of burial, resulting in moderately sensitive dating for this time period, but was too gradual over longer time scales to provide reliable dates. This dating scheme is potentially useful since other scientific dating techniques, for instance radiocarbon dating, are not workable on relatively young bioartefacts.

Desiccation of a body, or mummification, can be intentional, as in the famous Egyptian mummies, or natural, as a result of harshly arid burial conditions. Perhaps surprisingly, the cause of mummification of some archaeological remains cannot be determined from inspection alone. This situation has led, in part, to the comparative examination of skin samples from mummified remains recovered from ancient burials in an arctic glacier [144], on the gelid plains of Greenland [86], from Egypt's 'Tomb of Two Brothers' [113], and from graves in the arid desert of Peru [73,85] in order to detect chemical indicators of natural and/or artificial mummification. By monitoring the relative intensities of Raman bands assigned to keratin (proteins) and fats (lipids), an assessment of the cause of mummification as well as the state of preservation of the body can be made. All the mummies appear to have suffered from some chemical digenesis of the skin tissue, despite an outward appearance of good preservation. Amide bands attributable to the skin keratins showed band broadening compared to those same bands in contemporary skin samples, indicating that changes in the protein secondary structure accompanied desiccation and aging. In one instance, the

detection of thenardite or salt cake (Na_2SO_4), an ancient embalming material, by FT-Raman microscopy proved that the mummification was achieved at least in part artificially. This evidence of embalming was accompanied by spectral indications of well preserved α-helix and β-sheet protein secondary structure in the skin, thus indicating a more successful preservation of the mummy [113]. Perhaps surprisingly, the spectra of skin from the 500-year-old Greenland mummies was more similar to that of the 5200-year-old glacier mummy than to that of modern skin [86]. This result suggests that most of the degradation occurs relatively quickly after the death and mummification of the body. Increased levels of lipid in some Peruvian mummy skin samples, as evidenced by more intense bands attributed to CH stretching and CH_2 wagging modes near 2850 and 1300 cm^{-1}, respectively, suggest that an exogenous compound such as an ointment or balm might have been used to embalm some of the Peruvian mummies prior to burial. This hypothesis, though controversial, is supported by additional spectroscopic evidence of somewhat improved preservation of protein structures in the Peruvian skin samples. Without more analyses indicating the natural variation in the level of preservation of these mummies, however, little more can be made of this observation. Potential problems with laser heating of darkly pigmented Peruvian mummy skin and enhanced fluorescence from its larger melanin content were noticed in the analysis of some mummies, indicating that the technique might not be universally applicable.

Other ancient burial rituals have also been examined by FT-Raman microscopy. One such instance is the identification of untreated and unadulterated haematite applied to bones from a 3000-year-old Brazilian midden burial [64]. This instance is also said to have involved the application of a preparative layer of limewash, as judged by the presence of a broad, ill-resolved doublet feature at approximately 790 cm^{-1} in the Raman spectrum of the samples. Such practice would imply more sophistication to the burial practice of bone painting than previously thought, but it remains contestable. Earlier work on calcium phosphate minerals, like those found in bone, has shown that a 1064 nm laser excites a fluorescence doublet at $\sim$790 cm^{-1} [135], which is likely to be the spectral feature suggested here as indicating a limewash layer.

Ivory has been a common material for fashioning useful and decorative objects throughout history. Knowledge of the animal source of ivory for an object can reveal important information regarding the ancient utilisation of biological resources, trade patterns, and craft practices. However, because ivory was often shaped into highly ornamented artefacts, many of the classical physical measurements, e.g. Shreger line patterns, used to classify the source species are unworkable. An extensive project has sought to discriminate rapidly between various ivory-bearing species based on their Raman spectra, as well as to detect the use of alternative materials such as bone or plastic in ancient and modern imitations [13,61,66,67,70,117]. Subtle variations exist between the Raman spectra of different elephant and mammoth species, primarily as regards the relative band intensities in the region 1000–1100 cm^{-1} [68]. An objective means of assigning ivory spectra to Asian and African elephants, mammoth, narwhal, wart hog, hippopotamus, sperm whale, and walrus has been proposed which involves methodical flow chart protocols [66] and chemometric algorithms [13,117]. In the latter method, the spectrum was divided into 10 distinct regions, each of which was subjected to principal components analysis. Identification of test samples was not completely accurate, although the technique does show promise. However, great caution must be exercised when applying these methods to real artefacts. Ivory has a complex laminar structure consisting of cementum, enamel, and dentine. Although the cementum and enamel are often worn away in mature elephants, their persistence in other ivory-bearing species is more common, potentially complicating accurate classification depending on where and how the spectra are collected from reference materials and artefacts [95]. Additionally, the chemical composition of ivory from a single animal species is also likely to be diverse, with structural changes being expected depending on the age, history, and condition of the animal. At present, the number of samples from each species that have been analysed is too small to allow an assessment of the natural spectral diversity of these ivories. Nevertheless, the detailed and non-destructive analysis of these bio-artefacts as well as those mentioned previously is an exciting development that promises to expand greatly our knowledge of ancient peoples, their cultural practices, and their utilisation of natural resources.

4. Conclusion

Modern Raman microscopy has shed the experimental and instrumental limitations that so greatly restricted its early usefulness and, as a result, it is now enjoying a catholic acceptance in the physical and chemical sciences. The number and diversity of the applications reviewed in this article attest to the potential roles that dispersive and FT-Raman microscopy can and do play in the archaeometry laboratory. The specific and non-destructive identification of minute quantities of material can provide the archaeologist with invaluable information regarding an artefact including its authenticity, provenience, manufacturing technology, trade patterns, state of preservation, and in some instances, approximate age. It is hoped that this review will spur further

interest in Raman microscopy among the archaeology community.

Acknowledgements

The Marshall Aid Commemoration Commission is acknowledged for the award of a Marshall Sherfield Postdoctoral Fellowship (to GDS). The EPSRC is also thanked for financial support. The authors are grateful for the helpful discussions with Drs. Lucia Burgio, David Smith, and Simon Hillson regarding this manuscript. Dr. Burgio is especially thanked for her assistance in collecting the data for Fig. 4.

References

[1] I.M. Bell, R.J.H. Clark, P.J. Gibbs, Raman spectroscopic library of natural and synthetic pigments (pre ~1850 AD), Spectrochimica Acta A 53 (1997) 2159–2179.
[2] S.E.J. Bell, E.S.O. Bourguignon, A.C. Dennis, J.A. Fields, J.J. McGarvey, K.R. Seddon, Identification of dyes on ancient Chinese paper samples using the subtracted shifted Raman spectroscopy method, Analytical Chemistry 72 (2000) 234–239.
[3] M.-C. Bernard, A. Hugot-Le-Goff, B.V. Thi, S.C. de Torresi, Electrochromic reactions in manganese oxides, I. Raman analysis, Journal of the Electrochemical Society 140 (1993) 3065–3070.
[4] A. Bertoluzza, P. Brasili, L. Castri, F. Facchini, C. Fagnano, A. Tinti, Preliminary results in dating human skeletal remains by Raman spectroscopy, Journal of Raman Spectroscopy 28 (1997) 185–188.
[5] A. Bertoluzza, S. Cacciari, G. Cristini, C. Fagnano, A. Tinti, Non-destructive 'in situ' Raman study of artistic glasses, Journal of Raman Spectroscopy 26 (1995) 751–755.
[6] R. Bertoncello, L. Milanese, U. Russo, D. Pedron, P. Guerriero, S. Barison, Chemistry of cultural glasses: the early Medieval glasses of Monselice's Hill (Padova, Italy), Journal of Non-Crystalline Solids 306 (2002) 249–262.
[7] M. Bicchieri, M. Nardone, P.A. Russo, A. Sodo, M. Corsi, G. Cristoforetti, V. Palleschi, A. Salvetti, E. Tognoni, Characterization of azurite and lazurite based pigments by laser induced breakdown spectroscopy and micro-Raman spectroscopy, Spectrochimica Acta B 56 (2001) 915–922.
[8] D. Bikiaris, Sister Daniilia, S. Sotiropoulou, O. Katsimbiri, E. Pavlidou, A.P. Moutsatsou, Y. Chryssoulakis, Ochre-differentiation through micro-Raman and micro-FTIR spectroscopies: application on wall paintings at Meteora and Mount Athos, Greece, Spectrochimica Acta A 56 (1999) 3–18.
[9] M. Bouchard, Evaluation des Capacités de la Microscopie Raman dans la Charactérisation Minéralogique et Physico-Chemique de Matériaux Archéologiques: Métaux, Vitraux & Pigments, PhD dissertation, Muséum National d'Histoire Naturelle, 2001.
[10] M. Bouchard, D.C. Smith, Evaluating Raman microscopy for the non-destructive archaeometry of corroded coins: a powerful technique for conservation studies, Asian Chemical Letters 5 (2001) 157–169.
[11] M. Bouchard, D.C. Smith, Archaeological and experimental stained glass: a non-destructive Raman microscopic (RM) study, ART 2002: Seventh International Conference on Non-destructive Testing and Microanalysis for the Diagnostics and Conservation of Cultural and Environmental Heritage, 2002, 152 pp.
[12] M. Bouchard, D.C. Smith, Catalogue of 45 reference Raman spectra of minerals concerning research in art history or archaeology, especially on corroded metals & coloured glass, Spectrochimica Acta A 59 (2003) 2247–2266.
[13] R.H. Brody, H.G.M. Edwards, A.M. Pollard, Chemometric methods applied to the differentiation of fourier-transform Raman spectra of ivories, Analytica Chimica Acta 427 (2001) 223–232.
[14] R.H. Brody, H.G.M. Edwards, A.M. Pollard, A study of amber and copal samples using FT-Raman spectroscopy, Spectrochimica Acta A 57 (2001) 1325–1338.
[15] R.H. Brody, H.G.M. Edwards, A.M. Pollard, Fourier transform-Raman spectroscopic study of natural resins of archaeological interest, Biopolymers 67 (2002) 129–141.
[16] C.J. Brooke, H.G.M. Edwards, J.K.F. Tait, The Bottesford blue mystery: a Raman spectroscopic study of post-Mediaeval glazed tiles, Journal of Raman Spectroscopy 30 (1999) 429–434.
[17] K.L. Brown, R.J.H. Clark, Analysis of pigmentary materials on the Vinland Map and Tartar relation by Raman microprobe spectroscopy, Analytical Chemistry 74 (2002) 3658–3661.
[18] K.L. Brown, R.J.H. Clark, Analysis of key Anglo-Saxon manuscripts (8th–11th) centuries) in the British Library: pigment identification by Raman microscopy, Journal of Raman Spectroscopy 35 (2004) 181–189.
[19] K.L. Brown, R.J.H. Clark, The Lindisfarne Gospels and two other 8th century Anglo-Saxon/Insular manuscripts: pigment identification by Raman microscopy, Journal of Raman Spectroscopy 35 (2004) 4–12.
[20] K.L. Brown, R.J.H. Clark, Three English Manuscripts post-1066 AD: pigment identification and palette comparisons by Raman microscopy, Journal of Raman Spectroscopy 35 (2004) 217–223.
[21] S. Bruni, F. Cariati, F. Casadio, L. Toniolo, Identification of pigments on a XV century illuminated parchment by Raman and FTIR microscopies, Spectrochimica Acta A 55 (1999) 1371–1377.
[22] P. Bruno, M. Caselli, M.L. Curri, P. Favia, C. Laganara, A. Traini, Surface examination of red painting on Medieval pottery from the South of Italy, Annali di Chimica - Roma 87 (1997) 539–553.
[23] L. Burgio, R.J.H. Clark, Comparative pigment analysis of six modern Egyptian papyri and an authentic one of the 13th century BC by Raman microscopy and other techniques, Journal of Raman Spectroscopy 31 (2000) 395–401.
[24] L. Burgio, R.J.H. Clark, Library of FT-Raman spectra of pigments, minerals, pigment media and varnishes, and supplement to library of Raman spectra of pigments with visible excitation, Spectrochimica Acta A 57 (2001) 1491–1521.
[25] L. Burgio, R.J.H. Clark, S. Firth, Raman spectroscopy as a means for the identification of Plattnerite (PbO_2), of lead pigments and of their degradation products, The Analyst 126 (2001) 222–227.
[26] T. Calligaro, S. Colinart, J.P. Poirot, C. Sudres, Combined external-beam PIXE and μ-Raman characterisation of garnets used in Merovingian jewellery, Nuclear Instruments & Methods in Physics Research Section B: Beam Interactions with Materials and Atoms 189 (2002) 320–327.
[27] J. Chalmers, P.R. Griffiths (Eds.), The Handbook of Vibrational Spectroscopy, Wiley, New York, 2001.
[28] T.D. Chaplin, R.J.H. Clark, D.R. Beech, Comparison of genuine (1851–1852 AD) and forged or reproduction Hawaiian missionary stamps using Raman microscopy, Journal of Raman Spectroscopy 33 (2002) 424–428.
[29] E. Ciliberto, G. Spoto (Eds.), Modern Analytical Methods in Art and Archaeology, Wiley, New York, 2000.
[30] D.A. Ciomartan, R.J.H. Clark, L.J. McDonald, M. Odlyha, Studies on the thermal decomposition of basic lead(II) carbonate by Fourier-transform Raman spectroscopy, X-ray diffraction and thermal analysis, Journal of the Chemical Society, Dalton Transactions (1996) 3639–3645.

[31] R.J.H. Clark, Pigment identification on Medieval manuscripts by Raman microscopy, Journal of Molecular Structure 347 (1995) 417–428.
[32] R.J.H. Clark, L. Curri, G.S. Henshaw, C. Laganara, Characterization of brown–black and blue pigments in glazed pottery fragments from Castel Fiorentino (Foggia, Italy) by Raman microscopy, X-ray photoelectron spectroscopy, Journal of Raman Spectroscopy 28 (1997) 105–109.
[33] R.J.H. Clark, M.L. Curri, The identification by Raman microscopy and X-ray diffraction of iron-oxide pigments and of the red pigments found on Italian pottery fragments, Journal of Molecular Structure 440 (1998) 105–111.
[34] R.J.H. Clark, M.L. Curri, C. Laganara, Raman microscopy: the identification of Lapis Lazuli on Medieval pottery fragments from the South of Italy, Spectrochimica Acta A 53 (1997) 597–603.
[35] R.J.H. Clark, T.J. Dines, Resonance Raman spectroscopy and its application to inorganic chemistry, Angewandte Chemie, International Edition in English 25 (1986) 131–158.
[36] R.J.H. Clark, T.J. Dines, M. Kurmoo, On the nature of the sulfur chromophores in ultramarine blue, green, violet, and pink and of the selenium chromophore in ultramarine selenium: characterization of radical anions by electronic and resonance Raman spectroscopy and the determination of their excited-state geometries, Inorganic Chemistry 22 (1983) 2766–2772.
[37] R.J.H. Clark, P.J. Gibbs, Non-destructive *in situ* study of ancient Egyptian faience by Raman microscopy, Journal of Raman Spectroscopy 28 (1997) 99–103.
[38] R.H. Clarke, S. Londhe, M.E. Womble, Low-resolution Raman spectroscopy as an analytical tool for organic liquids, Spectroscopy 13 (1998) 28–35.
[39] R.J.H. Clark, J. van der Weerd, Identification of pigments and gemstones on the Tours Gospel: the early Carolingian Palette, Journal of Raman Spectroscopy 35 (2004) 279–283.
[40] E.E. Coleyshaw, W.P. Griffith, R.J. Bowell, Fourier-transform Raman spectroscopy of minerals, Spectrochimica Acta A 50 (1994) 1909–1918.
[41] P. Colomban, Lapis lazuli as unexpected blue pigment in Iranian lâjvardina ceramics, Journal of Raman Spectroscopy 34 (2003) 420–423.
[42] P. Colomban, G. March, L. Mazerolles, T. Karmous, N. Ayed, A. Ennabli, H. Slim, Raman identification of materials used for jewellery and mosaics in Ifriqiya, Journal of Raman Spectroscopy 34 (2003) 205–213.
[43] P. Colomban, G. Sagon, X. Faurel, Differentiation of antique ceramics from the Raman spectra of their coloured glazes and paintings, Journal of Raman Spectroscopy 32 (2001) 351–360.
[44] P. Colomban, F. Treppoz, Identification and differentiation of ancient and modern European porcelains by Raman macro- and micro-spectroscopy, Journal of Raman Spectroscopy 32 (2001) 93–102.
[45] P. Colomban, C. Truong, Non-Destructive Raman Study of the Glazing Technique in Lustre Potteries and Faience (9th–14th Centuries): Silver Ions, Nanoclusters, Microstructures, and Processing, Journal of Raman Spectroscopy 35 (2004) 195–207.
[46] P. Colomban, N.Q. Liem, G. Sagon, H.X. Tinh, T.B. Hoành, Microstructure, Composition, and Processing of 15th Century Vietnamese Porcelains and Celadons, Journal of Cultural Heritage 4 (2003) 187–197.
[47] C. Coupry, Application of Raman microspectrometry to art objects, Analusis 28 (2000) 39–46.
[48] G.A. Cox, B.A. Ford, The long-term corrosion of glass by groundwater, Journal of Materials Science 28 (1993) 5637–5647.
[49] A. Derbyshire, R. Withnall, Pigment analysis of portrait miniatures using Raman microscopy, Journal of Raman Spectroscopy 30 (1999) 185–188.
[50] H.G.M. Edwards, FT-Raman spectroscopic study of keratotic materials: horn, hoof and tortoiseshell, Spectrochimica Acta A 54 (1998) 745–757.
[51] H.G.M. Edwards, Raman microscopy in art and archaeology: illumination of historical mysteries in rock art and frescoes, Spectroscopy 17 (2002) 16–40.
[52] H.G.M. Edwards, L.F.C. de Oliveira, M. Nesbitt, Fourier-transform Raman characterization of brazilwood trees and substitutes, The Analyst 128 (2003) 82–87.
[53] H.G.M. Edwards, L. Drummond, J. Russ, Fourier-transform Raman spectroscopic study of pigments in Native American Indian rock art: Seminole canyon, Spectrochimica Acta A 54 (1998) 1849–1856.
[54] H.G.M. Edwards, L. Drummond, J. Russ, Fourier transform Raman spectroscopic study of prehistoric rock paintings from the Big Bend Region, Texas, Journal of Raman Spectroscopy 30 (1999) 421–428.
[55] H.G.M. Edwards, E. Ellis, D.W. Farwell, R.C. Janaway, Preliminary study of the application of Fourier transform Raman spectroscopy to the analysis of degraded archaeological linen textiles, Journal of Raman Spectroscopy 27 (1996) 663–669.
[56] H.G.M. Edwards, M.J. Falk, Fourier transform Raman spectroscopic study of ancient resins: a feasibility study of application to archaeological artefacts, Journal of Raman Spectroscopy 28 (1997) 211–218.
[57] H.G.M. Edwards, M.J. Falk, Fourier-transform Raman spectroscopic study of frankincense and myrrh, Spectrochimica Acta A 53 (1997) 2393–2401.
[58] H.G.M. Edwards, M.J. Falk, Investigation of the degradation products of archaeological linens by Raman spectroscopy, Applied Spectroscopy 51 (1997) 1134–1138.
[59] H.G.M. Edwards, M.J. Falk, M.G. Sibley, J. Alvarez-Benedi, F. Rull, FT-Raman spectroscopy of gums of technological significance, Spectrochimica Acta A 54 (1998) 903–920.
[60] H.G.M. Edwards, M.J.P. Falk, Fourier-transform Raman spectroscopic study of unsaturated and saturated waxes, Spectrochimica Acta A 53 (1997) 2685–2694.
[61] H.G.M. Edwards, D.W. Farwell, Ivory and simulated ivory artefacts: fourier transform Raman diagnostic study, Spectrochimica Acta A 51 (1995) 2073–2081.
[62] H.G.M. Edwards, D.W. Farwell, Fourier transform-Raman spectroscopy of amber, Spectrochimica Acta A 52 (1996) 1119–1125.
[63] H.G.M. Edwards, D.W. Farwell, L. Daffner, Fourier-transform Raman spectroscopic study of natural waxes and resins. 1, Spectrochimica Acta A 52 (1996) 1639–1648.
[64] H.G.M. Edwards, D.W. Farwell, D.L.A. de Faria, A.M.F. Monteiro, M.C. Afonso, P. De Blasis, S. Eggers, Raman spectroscopic study of 3000-year-old human skeletal remains from a Sambaqui, Santa Catarina, Brazil, Journal of Raman Spectroscopy 32 (2001) 17–22.
[65] H.G.M. Edwards, D.W. Farwell, C.P. Heron, H. Croft, A.R. David, Cats' eyes in a new light: Fourier transform Raman spectroscopic and gas chromatographic-mass spectrometric study of Egyptian mummies, Journal of Raman Spectroscopy 30 (1999) 139–146.
[66] H.G.M. Edwards, D.W. Farwell, J.M. Holder, E.E. Lawson, Fourier-transform Raman spectra of ivory III: identification of mammalian specimens, Spectrochimica Acta A 53 (1997) 2403–2409.
[67] H.G.M. Edwards, D.W. Farwell, J.M. Holder, E.E. Lawson, Fourier-transform Raman spectroscopy of ivory: II. Spectroscopic analysis and assignments, Journal of Molecular Structure 435 (1997) 49–58.
[68] H.G.M. Edwards, D.W. Farwell, J.M. Holder, E.E. Lawson, Fourier transform-Raman spectroscopy of ivory: a non-destructive diagnostic technique, Studies in Conservation 43 (1998) 9–16.

[69] H.G.M. Edwards, D.W. Farwell, A. Quye, 'Dragon's blood' I—characterization of an ancient resin using Fourier transform Raman spectroscopy, Journal of Raman Spectroscopy 28 (1997) 243–249.
[70] H.G.M. Edwards, D.W. Farwell, T. Seddon, J.K.F. Tait, Scrimshaw: real or fake? A Fourier-transform Raman diagnostic study, Journal of Raman Spectroscopy 26 (1995) 623–628.
[71] H.G.M. Edwards, D.W. Farwell, D. Webster, FT Raman microscopy of untreated natural plant fibres, Spectrochimica Acta A 53 (1997) 2383–2392.
[72] H.G.M. Edwards, D.W. Farwell, D.D. Wynn-Williams, FT-Raman spectroscopy of avian mummified tissue of archaeological relevance, Spectrochimica Acta A 55 (1999) 2691–2703.
[73] H.G.M. Edwards, M. Gniadecka, S. Petersen, J.P.H. Hansen, O.F. Nielsen, D.H. Christensen, H.C. Wulf, NIR-FT Raman spectroscopy as a diagnostic probe for mummified skin and nails, Vibrational Spectroscopy 28 (2002) 3–15.
[74] H.G.M. Edwards, E.M. Newton, J. Russ, Raman spectroscopic analysis of pigments and substrata in prehistoric rock art, Journal of Molecular Structure 550–551 (2000) 245–256.
[75] H.G.M. Edwards, M.G. Sibley, C. Heron, FT-Raman spectroscopic study of organic residues from 2300-year-old Vietnamese burial jars, Spectrochimica Acta A 53 (1997) 2373–2382.
[76] H.G.M. Edwards, J.K.F. Tait, FT-Raman spectroscopic study of decorated stained glass, Journal of Raman Spectroscopy 52 (1998) 679–682.
[77] H.G.M. Edwards, S.E.J. Villar, A.R. David, D.L.A. de Faria, Nondestructive Analysis of Ancient Egyptian Funerary Relics by Raman Spectroscopic Techniques, Analytica Chimica Acta 503 (2004) 223–233.
[78] H.G.M. Edwards, A.C. Williams, D.W. Farwell, Paleodental studies using FT-Raman spectroscopy, Biospectroscopy 1 (1995) 29–36.
[79] D.L.A. de Faria, F.N. Lopes, Natural Hematite or Heated Goethite: Can Raman Microscopy Differentiate Them? in: J. Mink, G. Jalsovszhy, G. Keresztury (Eds.), XVIIIth International Conference on Raman Spectroscopy, Wiley, New York, 2002, pp. 825–826.
[80] D.L.A. de Faria, V. Silva, M.T. de Oliveira, Raman microspectroscopy of some iron oxides and oxyhydroxides, Journal of Raman Spectroscopy 28 (1997) 873–878.
[81] X. Faurel, A. Vanderperre, P. Colomban, Pink pigment optimization by resonance Raman spectroscopy, Journal of Raman Spectroscopy 34 (2003) 290–294.
[82] R.L. Frost, W. Martens, J.T. Kloprogge, P.A. Williams, Raman spectroscopy of the basic copper chloride minerals atacamite and paratacamite: implications for the study of copper, brass and bronze objects of archaeological significance, Journal of Raman Spectroscopy 33 (2002) 801–806.
[83] R.L. Frost, P.A. Williams, W. Martens, J.T. Kloprogge, Raman spectroscopy of the polyatomic copper(II) minerals buttgenbachite and connellite: implications for studies of ancient copper objects and bronzes, Journal of Raman Spectroscopy 33 (2002) 752–757.
[84] F. Gendron, D.C. Smith, A. Gendron-Badou, Discovery of jadeite-jade in Guatemala confirmed by non-destructive Raman microscopy, Journal of Archaeological Sciences 29 (2002) 837–851.
[85] M. Gniadecka, H.G.M. Edwards, J.P.H. Hansen, O.F. Nielsen, D.H. Christensen, S.E. Guillen, H.C. Wulf, Near-infrared Fourier transform Raman spectroscopy of the mummified skin of the Alpine iceman, Qilakitsoq Greenland mummies and Chiribaya mummies from Peru, Journal of Raman Spectroscopy 30 (1999) 147–153.
[86] M. Gniadecka, H.C. Wulf, O.F. Nielsen, D.H. Christensen, J.P.H. Hansen, Fourier transform Raman spectroscopy of 15th century mummies from Qilakitsoq, Greenland, Journal of Raman Spectroscopy 28 (1997) 179–184.
[87] W.P. Griffith, Advances in the Raman and infrared spectroscopy of minerals, in: R.J.H. Clark, R.E. Hester (Eds.), Spectroscopy of Inorganic-Based Materials, Wiley, Chichester, 1987, pp. 119–188.
[88] B. Guineau, Non-destructive analysis of organic pigments and dyes using Raman microprobe, microfluorometer, or absorption microspectrometer, Studies in Conservation 34 (1989) 38–44.
[89] B. Guineau, Experiments in the identification of colorants *in situ*: possibilities and limitations, Dyes in History and Archaeology 10 (1992) 55–59.
[90] B. Guineau, M. Lorblanchet, B. Gratuze, L. Dulin, P. Roger, R. Akrich, F. Muller, Manganese black pigments in prehistoric paintings: the case of the Black Frieze of Pech Merle (France), Archaeometry 43 (2001) 211–225.
[91] H.A. Hänni, B. Schubiger, L. Kiefert, S. Häberli, Raman investigations on two historical objects from Basel Cathedral: the Reliquary Cross and Dorothy Monstrance, Gems & Gemology 34 (1998) 102–125.
[92] C.M. Harris, Raman revisited, Analytical Chemistry 57 (2002) 433A–438A.
[93] S.D. Harvey, T.J. Peters, B.W. Wright, Safety considerations for sample analysis using a near-infrared (785 nm) Raman laser source, Applied Spectroscopy 57 (2003) 580–587.
[94] P. Hendra, C. Jones, G. Warnes, Fourier Transform Raman Spectroscopy: Instrumentation and Chemical Applications, Ellis Horwood, Chichester, 1991.
[95] S. Hillson, Personal communication, 2001.
[96] F.J. Hunter, J.G. McDonnell, A.M. Pollard, C.R. Morris, C.C. Rowlands, The scientific identification of archaeological jet-like artefacts, Archaeometry 35 (1993) 69–89.
[97] A. Jurado-Lopez, O. Demko, R.J.H. Clark, D. Jacobs, Analysis of the palette of a precious 16th century illuminated Turkish manuscript by Raman microscopy, Journal of Raman Spectroscopy 35 (2004) 119–124.
[98] L. Kiefert, H. Hänni, T. Ostertag, Raman spectroscopic applications to gemmology, in: I.R. Lewis, H.G.M. Edwards (Eds.), Handbook of Raman Spectroscopy, Marcel Dekker, New York, 2001, pp. 469–489.
[99] M.T. Kirchner, H.G.M. Edwards, D. Lucy, A.M. Pollard, Ancient and modern specimens of human teeth: a Fourier transform Raman spectroscopic study, Journal of Raman Spectroscopy 28 (1997) 171–178.
[100] B.P. Lenain, Analytical Raman spectroscopy: a new generation of instruments, Analusis 28 (2000) 11–14.
[101] N.Q. Liem, G. Sagon, V.X. Quang, H.V. Tan, P. Colomban, Raman study of the microstructure, composition and processing of ancient Vietnamese (proto)porcelains and celadons (13–16th centuries), Journal of Raman Spectroscopy 31 (2000) 933–942.
[102] N.Q. Liem, N.T. Thanh, P. Colomban, Reliability of Raman micro-spectroscopy in analysing ancient ceramics: the case of ancient Vietnamese porcelain and celadon glazes, Journal of Raman Spectroscopy 33 (2002) 287–294.
[103] D.A. Long, The Raman Effect, Wiley, Chichester, 2002.
[104] W. Martens, R.L. Frost, J.T. Kloprogge, P.A. Williams, Raman spectroscopic study of the basic copper sulphates—implications for copper corrosion and 'bronze disease', Journal of Raman Spectroscopy 34 (2003) 145–151.
[105] E.J. Mawk, M. Hyman, M.W. Rowe, Re-examination of ancient DNA in Texas rock paintings, Journal of Archaeological Sciences 29 (2002) 301–306.
[106] L.I. McCann, K. Trentelman, T. Possley, B. Golding, Corrosion of ancient Chinese bronze money trees studied by Raman microscopy, Journal of Raman Spectroscopy 30 (1999) 121–132.
[107] L. Nasdala, A. Banerjee, T. Hager, W. Hofmeister, Laser Raman micro-spectroscopy in mineralogical research, Microscopy and Microanalysis March (2001) 11–13.
[108] L.F.C. de Oliveira, H.G.M. Edwards, R.L. Frost, J.T. Kloprogge, P.S. Middleton, Caput mortuum: spectroscopic and

structural studies of an ancient pigment, The Analyst 127 (2002) 536–541.
[109] S. Pagès-Camagna, S. Colinart, C. Coupry, Fabrication processes of archaeological Egyptian blue and green pigments enlightened by Raman microscopy and scanning electron microscopy, Journal of Raman Spectroscopy 30 (1999) 313–317.
[110] A. Paipetis, C. Vlattas, C. Galiotis, Remote laser Raman microscopy (ReRaM). 1—design and testing of a confocal microprobe, Journal of Raman Spectroscopy 27 (1996) 519–526.
[111] A. Perardi, L. Appolonia, P. Mirti, Non-destructive in situ determination of pigments in 15th century wall paintings by Raman microscopy, Analytica Chimica Acta 480 (2003) 317–325.
[112] A. Perardi, A. Zoppi, E. Castellucci, Micro-Raman spectroscopy for standard and in situ characterisation of painting materials, Journal of Cultural Heritage 1 (2000) S269–S272.
[113] S. Petersen, O.F. Nielsen, D.H. Christensen, H.G.M. Edwards, D.W. Farwell, R. David, P. Lambert, M. Gniadecka, H.C. Wulf, Near-infrared Fourier transform Raman spectroscopy of skin samples from the 'Tomb of the Two Brothers', Khnum-Nakht and Nekht-Ankh, XIIth dynasty Egyptian mummies (ca 2000 BC), Journal of Raman Spectroscopy 34 (2003) 375–379.
[114] J.P. Pretola, A feasibility study using silica polymorph ratios for sourcing chert and chalcedony lithic materials, Journal of Archaeological Sciences 28 (2001) 721–739.
[115] J. Russ, W.D. Kaluarachchi, L. Drummond, H.G.M. Edwards, The nature of a whewellite-rich rock crust associated with pictographs in southwestern Texas, Studies in Conservation 44 (1999) 91–103.
[116] J. Russ, R.L. Palma, D. Loyd, D.W. Farwell, H.G.M. Edwards, Analysis of the rock accretions in the Lower Pecos Region of southwest Texas, Geoarchaeology 10 (1995) 43–63.
[117] M. Shimoyama, T. Ninomiya, Y. Ozaki, Nondestructive Discrimination of Ivories and Prediction of Their Specific Gravity by Fourier-Transform Raman Spectroscopy and Chemometrics, The Analyst 128 (2003) 950–953.
[118] A. Sodo, M. Nardone, A. Ajò, G. Pozza, M. Bicchieri, Optical and Structural Properties of Gemmological Materials Used in Works of Art and Handicraft, Journal of Cultural Heritage 4 (2003) 317s–320s.
[119] D.C. Smith, Letting loose a laser: MRM (Mobile Raman Microscopy) for archaeometry and ethnomineralogy in the next millennium, Mineralogical Society Bulletin 125 (1999) 3–8.
[120] D.C. Smith, Pigments Rouges et Bleus sur Cinq Oeuvres d'Amérique: Analyse Non-destructive par MRM (Microscopie Raman Mobile), Techne 11 (2000) 69–83.
[121] D.C. Smith, A. Barbet, A Preliminary Raman Microscopic Exploration of Pigments in Wall Paintings in the Roman Tomb Discovered at Kertch, Ukraine, in 1891, Journal of Raman Spectroscopy 30 (1999) 319–324.
[122] D.C. Smith, M. Bouchard, M. Lorblanchet, An initial Raman microscopic investigation of prehistoric rock art in caves of the Quercy District, S.W. France, Journal of Raman Spectroscopy 30 (1999) 347–354.
[123] D.C. Smith, C. Carabatos-Nedelec, Raman spectroscopy applied to crystals: phenomena and principles, concepts and conventions, in: I. Lewis, H.G.M. Edwards (Eds.), A Handbook on Raman Spectroscopy, Marcel Dekker, New York, 2001, pp. 349–422.
[124] D.C. Smith, C. Carabatos-Nedelec, M. Bouchard, VITRORAMAN: establishing a database on the Raman spectra of pigments on and in stained glass. GEORAMAN'99, 1999, pp. 36–37.
[125] D.C. Smith, F. Gendron, Archaeometric application of the Raman microprobe to the non-destructive identification of two pre-Columbian ceremonial polished 'greenstone' axe-heads from Mesoamerica, Journal of Raman Spectroscopy 28 (1997) 731–738.
[126] D.C. Smith, S. Robin, Early Roman empire intaglios from 'rescue excavations' in Paris: an application of the Raman microprobe to the non-destructive characterization of archaeological objects, Journal of Raman Spectroscopy 28 (1997) 189–193.
[127] D.C. Smith, J.D. Vernioles, The temperature of fusion of a Celtic vitrified fort: a feasibility study of the non-destructive characterization of unprepared archaeological objects, Journal of Raman Spectroscopy 28 (1997) 195–197.
[128] G.D. Smith, R.J.H. Clark, Raman microscopy in art history and conservation science, Reviews in Conservation 2 (2001) 92–106.
[129] G.D. Smith, R.J.H. Clark, The role of H_2S in pigment blackening, Journal of Cultural Heritage 3 (2002) 101–105.
[130] G.D. Smith, A. Derbyshire, R.J.H. Clark, *In situ* spectroscopic detection of PbS on a blackened manuscript illumination by Raman microscopy, Studies in Conservation 47 (2002) 250–256.
[131] R.J. Speakman, H. Neff, Evaluation of painted pottery from the Mesa Verde region using laser ablation-inductively coupled plasma-mass spectrometry (LA-ICP-MS), American Antiquity 67 (2002) 137–144.
[132] J.D. Stewart, K.R. Adams, Evaluating visual criteria for identifying carbon- and iron-based pottery paints from the Four Corners Region using SEM–EDS, American Antiquity 64 (1999) 675–696.
[133] J.D. Stewart, K.R. Adams, G.J. Borradaile, A.J. MacKenzie, Investigations of paints on ancestral Puebloan black-on-white pottery using magnetic and microanalysis methods, Journal of Archaeological Sciences 29 (2002) 1309–1316.
[134] K. Trentelman, L. Stodulski, D. Scott, M. Back, S. Stock, D. Strahan, A.R. Drews, A. O'Neill, W.H. Weber, A.E. Chen, S.J. Garrett, The characterization of a new pale blue corrosion product found on copper alloy artifacts, Studies in Conservation 47 (2002) 217–227.
[135] H. Tsuda, J. Arias, B. Leon, J. Arends, Necessary precautions in the Raman analysis of calcium phosphate minerals using 1.06 μm YAG laser excitation, Applied Spectroscopy 52 (1998) 1122–1126.
[136] G. Turrell, J. Corset (Eds.), Raman Microscopy: Developments and Applications, Academic Press, London, 1996.
[137] P. Vandenabeele, L. Moens, H.G.M. Edwards, R. Dams, Raman spectroscopic database of azo pigments and application to modern art studies, Journal of Raman Spectroscopy 31 (2000) 509–517.
[138] P. Vandenabeele, B. Wehling, L. Moens, H. Edwards, M. De Reu, G. Van Hooydonk, Analysis with micro-Raman spectroscopy of natural organic binding media and varnishes used in art, Analytica Chimica Acta 407 (2000) 261–274.
[139] C. Wang, B. Lu, J. Zuo, S. Zhang, S. Tan, M. Suzuki, W.T. Chase, Structural and elemental analysis of the nanocrystalline SnO_2 in the surface of ancient Chinese black mirrors, Nanostructured Materials 5 (1995) 489–496.
[140] X. Wang, C. Wang, J. Yang, L. Chen, J. Feng, M. Shi, Study of Wall-Painting Pigments from Feng Hui Tomb by Raman Spectroscopy and High-Resolution Electron Microscopy, Journal of Raman Spectroscopy 35 (2004) 274–278.
[141] J. van der Weerd, S. Firth, R.J.H. Clark, T. Rehren, Identification of iron oxide impurities in early industrial-scale processed platinum: the three Rouble Russian coin of 1837, Materials Characterization, submitted for publication.
[142] J. van der Weerd, G.D. Smith, S. Firth, R.J.H. Clark, Identification of black pigments on prehistoric southwest American potsherds by infrared and Raman microscopy, Journal of Archaeological Sciences, in press.
[143] H.G. Wiedemann, E. Arpagaus, D. Müller, C. Marcolli, S. Weigel, A. Reller, Pigments of the bust of Nefertete compared with those of the Karnak Talatats, Thermochimica Acta 382 (2002) 239–247.

[144] A.C. Williams, H.G.M. Edwards, B.W. Barry, The 'iceman': molecular structure of 5200-year-old skin characterised by Raman spectroscopy and electron microscopy, Biochimica et Biophysica Acta 1246 (1995) 98–105.
[145] A.A. Wilson, H.G.M. Edwards, D.W. Farwell, R.C. Janaway, Fourier transform Raman spectroscopy: evaluation as a non-destructive technique for studying the degradation of human hair from archaeological and forensic environments, Journal of Raman Spectroscopy (1999) 367–373.
[146] M. Windholz (Ed.), The Merck Index, Merck & Co., Inc., Rahway, N.J., 1976.
[147] W. Winkler, E.C. Kirchner, A. Asenbaum, M. Musso, A Raman spectroscopic approach to the maturation process of fossil resins, Journal of Raman Spectroscopy 32 (2001) 59–63.
[148] R. Withnall, R.J.H. Clark, C.J. Cooksey, M.A.M. Daniels, Non-destructive, in situ identification of indigo/woad and shellfish purple by Raman microscopy and visible reflectance spectroscopy, Dyes in History and Archaeology 11 (1993) 19–24.
[149] R. Withnall, A. Derbyshire, S. Thiel, M.J. Hughes, Raman microscopic analysis in museology, Proceedings of the International Society for Optical Engineering 4098 (2000) 217–231.
[150] B. Wopenka, R. Popelka, J.D. Pasteris, S. Rotroff, Understanding the mineralogical composition of ancient Greek pottery through Raman microprobe spectroscopy, Applied Spectroscopy 56 (2002) 1320–1328.
[151] A. Zoppi, C. Lofrumento, E.M. Castellucci, M.G. Migliorini, Micro-Raman technique for phase analysis on archaeological ceramics, Spectroscopy Europe 14 (2002) 16–21.
[152] A. Zoppi, G.F. Signorini, F. Lucarelli, L. Bachechi, Characterisation of painting materials from Eritrea rock art sites with non-destructive spectroscopic techniques, Journal of Cultural Heritage 3 (2002) 299–308.
[153] J. Zuo, C. Wang, C. Xu, Non-destructive in situ study of white and black coating on painted pottery sherds from Bancun Site (Henan, China) by Raman microscopy, Spectroscopy Letters 31 (1998) 1431–1440.
[154] J. Zuo, C. Wang, C. Xu, P. Qiu, G. Xu, H. Zhao, Raman microscopy study of the pigments on the ancient wall painting from the large grave in Wanzhang (Hebei, China), Spectroscopy Letters 32 (1999) 841–850.
[155] J. Zuo, C. Xu, C. Wang, Z. Yushi, Identification of the pigment in painted pottery from the Xishan site by Raman microscopy, Journal of Raman Spectroscopy 30 (1999) 1053–1055.
[156] J. Zuo, X. Zhao, R. Wu, G. Du, C. Xu, C. Wang, Analysis of the pigments on painted pottery figurines from the Han Dynasty's Yangling tombs by Raman microscopy, Journal of Raman Spectroscopy 34 (2003) 121–125.